

Instituto Tecnológico y de Estudios Superiores de Monterrey

Campus Monterrey

School of Engineering and Sciences



Manufacturability of PLA Parts Reinforced with TiO_2 Nanoparticles by
Ultrasonic Molding.

A thesis presented by

Mariana Macías Naranjo

Submitted to the
School of Engineering and Sciences
in partial fulfillment of the requirements for the degree of

Master of Science

In

Manufacturing Systems

Monterrey Nuevo León, June 16th, 2020

Dedication

*To **God**, who always guides me, gives me peace and strength, and blesses me in so many ways. Without Him, nothing is possible.*

*To my parents, **Arturo Macías Aguilar**, and **Nydia Naranjo Fuentes**, who encouraged me to continue studying, to give my best, to believe in me and not to be redeemed. Thank you for all your advice, your words, your company, your efforts, your help and for giving me the resources to complete this opportunity. This was possible, thanks to you.*

Acknowledgements

*I thank **God** for being my engine of life, for the opportunity to end this stage with so many blessings and for always giving me the strength to keep going.*

*I thank **my parents, Nydia and Arturo, and my brother, Arturo**, for always being present in my life and being my strength, my support, and my motivation not to give up.*

*To **Dr. Elisa Virginia Vázquez Lepe** and to **Dr. Inés Ferrer Real** for being excellent advisers, for guiding to carry out all the work, always trying to perfect every detail and for supporting me at this stage.*

*I thank **the committee members** for their valuable insights, to improve the work. To **Dr. Wendy de Lourdes Ortega Lara** for the support for conducting tests in the laboratory and for teaching me to understand the behavior of materials. To **Dr. Ciro Angel Rodríguez González** for his criticism to highlight important aspects of the work.*

*I thank to **LCQ. Regina Elizabeth Vargas Mejía** for the support in carrying out tests in the laboratory and teaching me the technique.*

*I would like to express my gratitude for the support provided at all times and for being very important people in my life. To **my grandmothers** and to **all my family**, to **my boyfriend, Gerardo García**, to **my friends**, to **my professors** and to **my classmates**.*

*For giving me your help and support in some aspects to carry out the thesis, I thank **Ulisses Alberto Heredia, Luis Cuevas, Ferran Serra and Andre Mazega**.*

*Finally, I thank the institutions for giving me the opportunity to successfully complete the thesis. To **Tecnológico de Monterrey** for giving me the opportunity to study a master degree, to **CONACyT** with the support for living, to **University of Girona, grEp** and **LEPAMAP**, for the knowledge provided and allowing me to carry out experimentation in their facilities.*

MANUFACTURABILITY OF PLA PARTS REINFORCED WITH TiO₂ NANOPARTICLES BY ULTRASONIC MOLDING

by

Mariana Macías Naranjo

Abstract

Ultrasonic molding is a new technology that makes it possible to manufacture micro parts by transforming mechanical energy into thermal energy by means of vibrations. Through this technology, polymers can be used, which are positioning themselves in an important place in the medical sector. Thanks to the advantages of ultrasonic molding, it allows the use of medical grade materials, avoiding waste, degradation and using complex geometries.

The company Ultrason, creator of the Sonorus 1G machine, updated the software used by the machine, in order to improve the stabilization of the process parameters. Among the updates, the centering of the sonotrode was improved with air valves, in addition to separating the parameters by phases of the process and providing the behavior of the manufacture of the parts through data sheets. Thanks to this, a methodology was established for the stabilization of process parameters, where phase by phase is worked and the outputs in each phase were evaluated. For each phase, successful outputs were established to detect which parameters work and which do not.

The experimental process was divided into three stages: Preliminary Experimentation, First Experimentation and Final Experimentation. Preliminary experimentation was performed based on the range of parameters proposed by the Ultrasonic Molding Handbook. The first experimentation was carried out using a 2^k experiment design and the outputs were evaluated. Finally, in the final experimentation, only some parameters were modified to improve the repeatability of the process. To analyze the experimental results, a statistical analysis was carried out with Minitab, to determine which parameters were significant in terms of the expected outputs in each phase. Process parameter windows were obtained.

On the other hand, the objective was to verify the manufacturability of PLA parts with nanoparticles of titanium dioxide (TiO₂). The material was mixed in three concentrations: 2.5, 5.0 and 7.5 wt. %. For the preparation of the blends, the material was mixed, milled and sieved. The appropriate size for the ultrasonic molding process was selected and the parameters obtained for the PLA were used as a base for experimentation. Results were evaluated and 20 samples were made for characterization. In the characterization, morphological, physical, chemical and mechanical properties were evaluated to determine the behavior of the TiO₂ nanoparticles in the PLA, as well as the influence of the ultrasonic molding process working with a reinforced material.

List of Figures

Figure 1. Sonorus 1G machine [37].....	15
Figure 2. Machine Components.....	16
Figure 3. Ultrasonic Molding Process.....	18
Figure 4. Mold with the two cavities.....	20
Figure 5. Tensile bar dimensions.....	20
Figure 6. Examples of Compactation Outputs.....	22
Figure 7. Example of Pre-heating Outputs (Cylinder Formation).....	23
Figure 8. Examples of Pre-heating Outputs (Melted Pellets).....	23
Figure 9. Examples of Melting Outputs.....	24
Figure 10. Examples of Filling Outputs.....	24
Figure 11. Examples of Expected Outputs.....	25
Figure 12. Experimental Procedure.....	26
Figure 13. Mixing Process.....	29
Figure 14. Milling Process.....	30
Figure 15. Sieving Process.....	30
Figure 16. Branson 2800 equipment.....	31
Figure 17. Quorum Q150R – Rotary Pumped Coater.....	32
Figure 18. Zeiss EVO-MA25 microscope.....	32
Figure 19. Ceast – Melt Flow Quick Index.....	33
Figure 20. Paralytical Emphyrean.....	33
Figure 21. PerkinElmer FT-IR / FIR Spectrometer.....	34
Figure 22. Instron 3365 Universal Testing Machine.....	35
Figure 23. Output in Compactation, a) Plunger Position for PA12 and b) Plunger Position for PLA.....	37
Figure 24. Outputs in Pre-heating, a) Outputs for PA12 and b) Outputs for PLA.....	38
Figure 25. Outputs in Melting.....	39
Figure 26. Outputs in Filling.....	39
Figure 27. Influence of the pellets.....	41
Figure 28. Pellets / Amplitude in Melting.....	41
Figure 29. Travel Change.....	42
Figure 30. Comparison of US Energy vs % Filled Piece.....	43
Figure 31. SEM Images of PLA/TiO ₂ nanoparticles.....	45
Figure 32. MFI with the increment of nanoparticles.....	47
Figure 33. XRD - Comparison between the different materials.....	48
Figure 34. Points of analysis.....	49
Figure 35. FTIR Spectra – Comparison between different analysis points.....	50
Figure 36. Homogeneity difference between the two points analyzed.....	50
Figure 37. FTIR Spectra – Comparison between different materials at the center.....	52
Figure 38. Tensile testing.....	53
Figure 39. Young’s Modulus and US Energy vs % of nanoparticles.....	54

List of Tables

Table 1. Ultrasonic Molding Parameters.....	18
Table 2. Phases with its parameters.	19
Table 3. Properties of the materials.	21
Table 4. Stages of the process with their outputs to evaluate.	22
Table 5. 2 ^k Factorial Design.....	28
Table 6. Significant Parameters for PA12.....	36
Table 7. Significant Parameters for PLA.	36
Table 8. First Process Parameters Window for PA12.	40
Table 9. First Process Parameters Window for PLA.....	40
Table 10. Travel Change Comparison.....	43
Table 11. Final Process Parameters Window for PA12.....	44
Table 12. Final Process Parameters Window for PLA.....	44
Table 13. Final Process Parameters Window for PLA/TiO ₂	44
Table 14. Melting Flow Index.	46
Table 15. Both phases for TiO ₂ : Rutile and Anatase.....	48
Table 16. Tensile Testing Analysis.	54
Table 17. Significant Parameters in Tensile Testing.....	54

Contents

Abstract	4
List of Figures	5
List of Tables	6
1. Introduction	9
1.1. Motivation.....	9
1.2. Problem Statement.....	9
1.3. Objectives	10
2. State of Art	11
3. Ultrasonic Molding Process	15
3.1. Presentation of Sonorus 1G machine.....	15
3.2. Description of the ultrasonic molding process.	15
3.3. Ultrasonic Molding Phases.....	16
3.4. Process parameters	18
4. Mold, geometry, and materials	19
4.1. Mold and geometry of the part.....	19
4.2. Materials	20
5. Methodology to stabilize parameters in USM	21
6. Experimentation with neat material: PA12 y PLA.	25
6.1. Preliminary Experimentation	26
6.2. First Experimentation	28
6.3. Final Experimentation	28
7. Experimentation with blends: PLA + TiO₂	29
7.1. Blends Preparation: Mixing, Milling and Sieving Process.	29
7.2. Experimental Procedure with Blends: PLA + TiO ₂	30
7.3. Parts Characterization Conditions.	31
7.3.1. <i>Scanning Electron Microscopy (SEM)</i>	31
7.3.2. <i>Melt Flow Index (MFI)</i>	32
7.3.3. <i>X-Ray Diffraction (XRD)</i>	33
7.3.4. <i>Fourier-Transform Infrared Spectroscopy (FTIR)</i>	34
7.3.5. <i>Tensile Testing</i>	34
8. Results and Discussion	35
8.1. Analysis of the Experimental Results	35
8.1.1. <i>Results in First Experimentation</i>	35
8.1.2. <i>Results in Final Experimentation</i>	40
8.2. Parts Characterization.....	44
8.2.1. <i>Scanning Electron Microscope (SEM)</i>	44

8.2.2. Melt Flow Index (MFI).....	46
8.2.3. X-Ray Diffraction XRD.....	47
8.2.4. Fourier-Transform Infrared Spectroscopy (FTIR).....	49
8.2.5. Tensile Test.....	52
9. Conclusions	55
Appendix A.....	57
Appendix B.....	57
Bibliography.....	58
Curriculum Vitae	61

1. Introduction

1.1. Motivation

The manufacture of micro parts made from polymer nanocomposites has increased in recent years. There are technologies that seek to manufacture these, such as micro injection molding. Despite the fact that this conventional technique offers great advantages such as high productivity, high repeatability and the use of complex geometries, it also has problems with material dosing and high residence times, which can lead to material degradation.

Due to this problem, new technologies are sought that allow the manufacture of microparts of polymer nanocomposites, avoiding waste and material degradation. Polymer nanocomposites have positioned themselves in an important place in the medical sector. Because of this, the materials used can become expensive and with specific properties that have to be taken care of in its processing. Ultrasonic Molding is a new technology for the manufacture of micro parts. However, it is a technology that is still under investigation.

The motivation of this work is to process polylactic acid (PLA) with nanoparticles of titanium dioxide (TiO_2) by ultrasonic molding in order to use this blend in a medical device in a future work. PLA is a biodegradable polymer that offers high biocompatibility, like TiO_2 , thanks to its low toxicity. The mixture of these materials provides new properties to be used in a medical device.

1.2. Problem Statement

As ultrasonic molding technology is still under investigation, there are still many fields to discover. With this technology, different polymers have been worked, analyzing the manufacturability of them, as well as polymer blends and few works have been carried out on polymer nanocomposites. However, the machine they used with this technology had many areas of opportunity to improve the process.

Currently, the company Ultrason, in charge of manufacturing the machines that use this technology, has developed a new software that allows establishing a methodology to

better control the phases of the process, as well as analyze the behavior in each of the phases and have less variability in the process. That is why, in addition to establishing a methodology using this technology, it is desired the processing of a new polymer nanocomposites in Ultrasonic Molding.

1.3. Objectives

The general objectives of this work are:

- To define and to validate a methodology for the stabilization of process parameters in ultrasonic molding.
- To analyze the manufacturability of PLA parts reinforced with TiO₂ nanoparticles in the ultrasonic molding process.

The specific objectives are:

- To determine the process parameters in each of the phases.
- To establish the expected outputs in each phase.
- To determine the influence of each of the parameters in each phase.
- To carry out a statistical analysis that provides conclusions on the influence of the parameters on each of the outputs.
- To define the process parameters window for each of the materials.
- To plan preparation of the blends.
- To verify the manufacturability of TiO₂ reinforced PLA parts with quantity of complete parts.
- To characterize the material to analyze the influence of the process and the increase in nanoparticles.

2. State of Art

In recent years, the interest in polymer nanocomposites has been increasing due to the potential that these mixtures offer regarding the improvement of their physical, chemical and mechanical properties, compared to neat polymers or mixtures of them. Due to these properties, these materials have been positioned in an important place in the medical sector.

For the manufacture of medical devices, made from polymer components, there are different technologies used for micropart molding, including hot stamping, micro injection molding (μ IM), reaction injection molding, compression molding and thermoformed [1]. Micro injection molding is one of the most widely used conventional techniques for the production of polymeric microparts thanks to its high productivity, cost-effectiveness ratio, high repeatability and the use of complex geometries [1]. However, the main drawback of this manufacturing technology is that it presents material dosing problems, that is, large amounts of material are wasted [2], residence times are high [3], possible material degradation [4][5], and limited geometries [6]. For this reason, new technologies emerge that seek to optimize the micropart molding process.

Ultrasonic Molding known as USM is a recent technology that has been developed and implemented as a good alternative to manufacture micro components for the medical sector. However, despite being an interesting alternative to conventional processes, it is still under investigation due to the difficulty of optimizing process parameters [7]. The main source of this technology is ultrasound generation, where mechanical energy is transformed into heat energy to mold the material. Among the advantages offered by USM technology are the reduction of material waste, low temperature process [8][9], different geometries with high surface quality [10][11], low residence time [12] and energy saving [13][14].

USM emerged in 2002 when Michaeli et al. [2] proposes the use of ultrasound to melt a small amount of material, inject it into a cavity and thus manufacture high quality micro components. Michaeli et al. [2][15][12], has contributed to great advances in technology. The first prototype of a machine using this technology was presented in 2006 [15] but the molding was of poor quality. In 2009, Bas et al. [16] patented the prototype ultrasound machine. However, in 2014, Puliga et al. [17] patented an improved version of the ultrasonic molding machine to position itself in the market [“Sonus” by Ultrasion S.L.).

Different works were carried out with this machine [13][18][19][20][21][22] and later, a configuration modification was made to decrease the flash and avoid solids inside the mold [23][14][24][25][11][26].

Since the establishment of these machines, the main parameters involved in the process have been studied. Some of them are specific for USM and their influence is not clearly distinguished in the results. The sonotrode, is the order of provides the vibrations to the material, known this parameter as the Amplitude. This parameter is considered one of the main parameters to find the optimal process window [3][13][27][28][29]. Because its importance is known, some authors decided to take it as a fixed value to study the other parameters [30][18][27]. It is important to bear in mind that when applying high amplitudes it can degrade the material [3] or instead, if it is low amplitudes, the pieces are not completed, because not all the material melted [31].

Another parameter is the force or pressure applied to push the material. If very high forces are used, unmelted material can be introduced into the cavity [12], thus obtaining incomplete parts. Grabalosa et al. [30] mention that using higher forces, they do not affect the mechanical properties.

Velocity is a parameter recently added to Sonorus machines, which is also related to the force applied to the material. The influence of this parameter is still being investigated since different results are obtained. Dorf et al. [27] mentions that, at low velocities, cavitation occurs at the end of the piece and at high velocities, higher mechanical strength is obtained but there are incomplete pieces. On the other hand, when processing polypropylene, Masato et al. [14] found no influence on the injection velocity. In contrast, Negre et al [18] mention that at higher velocities, better filling results.

Another parameter is the ultrasound time, as its name indicates; it is the time that vibrations are applied to the material. For some authors [3][13][29] it is considered a main factor. Grabalosa et al. [30] shows that the ultrasound time has a great impact on the filling of the piece. It is important to note that if the material has already melted completely and vibrations continue to be applied longer, it may degrade [25]. Janer et al. [7] concludes that at shorter ultrasound times, incomplete parts are produced and at higher times, the material degrades.

Finally, another of the mentioned parameters is the shape of the raw material. The raw material can be presented in pellets, powder, filaments, among other presentations. According to Sánchez-Sánchez et al. [28] they mention that it is the most important factor. In this process, it is very important how the pellets are arranged, because the friction generated between them is what melts them. Montes et al. [32] concluded that the smaller the pellets, the lower the temperature needed for casting. This is related to the fact that the powder presentation requires less amplitude [13].

There are other factors that affect the process indirectly and have not been studied in depth. Sánchez-Sánchez et al. [23] indicated that the mold temperature is related to obtain good tensile strength. Another factor, according to Heredia et al. [10] are the venting holes that have a function for filling the specimen. Negre et al. [18] indicate that the drying of the pellets is necessary before being processed to decrease porosity. Another important aspect is the position of the heaters in the mold for the correct filling of the specimen.

To determine the importance of all the parameters and factors mentioned, an experiment design must be carried out that allows them to be related to the process responses. At the end of the process, the desired geometry, adequate mechanical properties and no signs of defects and impurities are sought [7]. The ability to obtain a complete piece has been studied by several authors using this technology [30][13][29][11]. The repeatability of the process is increased depending on the nature of the polymer such as PP [18] or PS [11], unlike other polymers the repeatability is less than for PPSU [27]. Also according to the parameters used, the filling varies. Several authors assure that the filling of the pieces occurs at low ultrasound times and low pressures [30][29]. Other authors report that a greater amplitude is required for the filling of the piece [3][30][27][28][26]. According to Ferrer et al. [11] report that at lower velocities, better filling results are obtained, unlike Dorf et al. [25], high velocity are required.

Through ultrasound molding, different polymers have been worked among them PA [30], PLA [13][29], PMMA [29], PP [18], UHMWPE [28][26], PPSU [27], PS [11] and PEEK [25]. Polypropylene (PP) was one of the first tested [12] and it was successfully used in the work of Negre et al. [18]. Another of the polymers used was polylactic acid (PLA) by a large number of authors [3][13][10][29][20]. Michaeli et al. [12][15] studied polyoxymethylene

(POM) and Janer et al. [33] with a recent study in, showed good results. PMMA has also been processed without degradation [29]. On the other hand, some nanocomposites have been processed with ultrasound [34][13][19][20][21][22].

PLA is a polymer of great interest to the medical sector due to its good compatibility, biodegradability and good mechanical properties. Thanks to this, it has been used in bone screws, surgical sutures, controlled drug delivery and tissue engineering [35]. On the other hand, TiO₂ nanoparticles have good chemical stability, good biocompatibility, low toxicity. The mixing of these materials is to improve impact toughness [35]. Furthermore, because PLA can be easily damaged, TiO₂ prevents possible degradation [36]. This mixture of materials has been investigated by different authors, but its processing by ultrasound molding technology has not yet been reported.

3. Ultrasonic Molding Process

3.1. Presentation of Sonorus 1G machine.

Ultrason - *Innovative Ultrasonic Solutions* is the manufacturing company of this technology located in Barcelona, Spain. The machine that was utilized for the experimentation was the Sonorus 1G (Figure 1) for micropart ultrasonic molding.



Figure 1. Sonorus 1G machine [37].

The technology focus in the manufacture of micro plastic parts in a small machine designed to use the least energy possible, optimize the properties of the molten plastic, reduce material waste and reduce the costs of contingent tools [38].

3.2. Description of the ultrasonic molding process.

The ultrasound system transforms high-frequency electrical vibrations into mechanical vibrations [37]. The converter is a piezoelectric element that expands and contracts at its resonant frequency (30Khz) when it is activated by electrical power. There are important components in charge of the process (Figure 2). The sonotrode is a part in charge of transfer the ultrasonic vibration to the introduced material [37].

The plunger presses the pellets against the sonotrode which transmits the high frequency vibrations. The vibrations are transformed into thermal energy through the friction generated between the surface of the pellets against the sonotrode, as well as the intermolecular heat generated. Due to this, the pellets begin to melt. Once melted, the material is pushed by the plunger, filling the mold cavity until it solidifies [37].

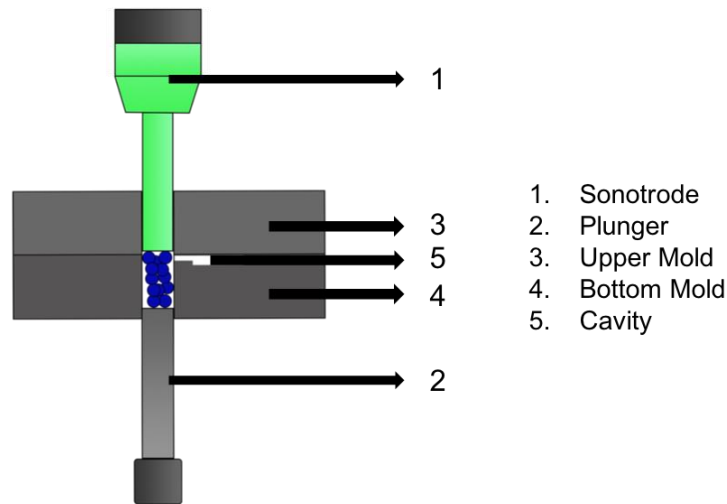


Figure 2. Machine Components.

3.3. Ultrasonic Molding Phases

For the USM process, the cycle is divided into 6 stages: Feeding, Compactation, Pre-heating, Melting, Filling and Cooling (Figure 3).

1. Feeding

The Sonorus equipment has a pellet dosing system that allows the quantification of pellets, according to the required mass depending on the volume of the mold. To calculate the required mass to introduce, it is necessary to obtain the volume of the cavity to be filled, considering leaving 2 mm of material in the part of the riser, as well as considering the density of the used material. Once it has the necessary mass, it is calculated in the number of pellets to be entered this parameter in the equipment. The more homogeneous the pellets, the Sonorus has a better repeatability with each shot.

2. Compactation

Through the sonotrode, the pellets are compacted by strokes impact, and it is established depending on the material to be used. This has the objective of creating a flat surface, in order to reduce tangential forces, since this can move the sonotrode from the center, thus generating leaks. On the other hand, since it has a flat surface, it allows the material to be homogenized and helps the following phases.

3. Pre-heating

During this phase, vibrations are applied to the previous compacted pellets by the sonotrode application, which generates heat, and consequently, the melted pellets create a cylinder. This stage allows to facilitate the melting stage, in order to reduce the applied energy and therefore, reduce the degradation of the material.

4. Melting

The sonotrode generates vibrations that allow the material, through friction, to generate heat and it could be melted. On the other hand, the piston applies a certain established pressure with the purpose of pushing the material and allowing the vibrations of the sonotrode to reach all the material, as well as introducing the material into the cavity. According to the update of the machine, this stage can be limited by time, by maximum force or by travel. Travel is a new parameter entered, and it refers to the distance traveled by the plunger.

5. Filling

For this stage, it is important to have done an appropriate job in the two previous stages, since otherwise, it would be difficult to achieve the objective at this stage. During this stage, the sonotrode stops vibrating, and the material is completely pushed into the cavity through pressure applied by the plunger. The 95% of the material must be introduced into the cavity to obtain a complete piece.

6. Cooling

It is the last stage of the process, where the material is kept for a certain time so that it reaches the desired temperature. This allows the material not to be deformed when unmolding the part.

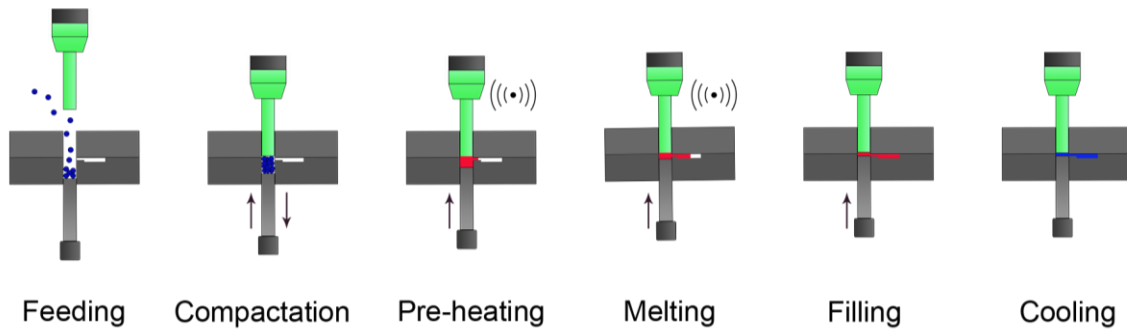


Figure 3. Ultrasonic Molding Process

3.4. Process parameters

Table 1 presents the parameters that are involved in the different phases of the process.

Table 1. Ultrasonic Molding Paramaters.

Parameters	Abbreviation	Units	Description
Amplitude	AV	%	Amplitude of vibrations provided by the sonotrode
Force	F	N	Force applied to the material by means of the plunger and sonotrode
Velocity	V	mm/s	Velocity with which the sonotrode or plunger travels
Plunger Position	PP	Mm	Position in which the plunger is located
Time	T	S	Phase time
Travel	Tr	Mm	Plunger displacement
Strokes	St	-	Shocks that the sonotrode applies to the material

Considering the 6 preceding phases, the Compactation, Pre-heating, Melting and Filling phases comprise the considered parameters for the experimentation that was carried out (Table 2).

Table 2. Phases with its parameters.

Phases	Parameters to vary
Compaction	Strokes
Pre-heating	Amplitude
	Force
	Time
Melting	Amplitude
	Force
	Velocity
	Travel or Time
Filling	Force
	Velocity
	Time

4. Mold, geometry, and materials.

4.1. Mold and geometry of the part.

The mold is made of 45NiCrMo16 precision flat steel, specifically made with HASCO plates reference K252 / 095x095x27 / 1.12767 [\[39\]](#).

The mold is mainly made up of two parts (Figure 4). The upper part is flat, and the lower part is where the cavity of the geometry to be manufactured is located. The cavity is designed to make two different pieces: One tensile bar or two plates. The mold has a locking system to inject the desired piece.

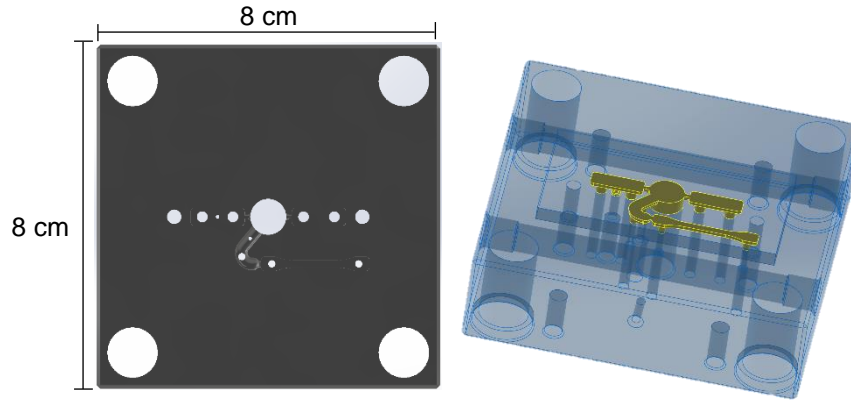


Figure 4. Mold with the two cavities.

The geometry for this work was tensile bar with the dimensions specified in Figure 5.

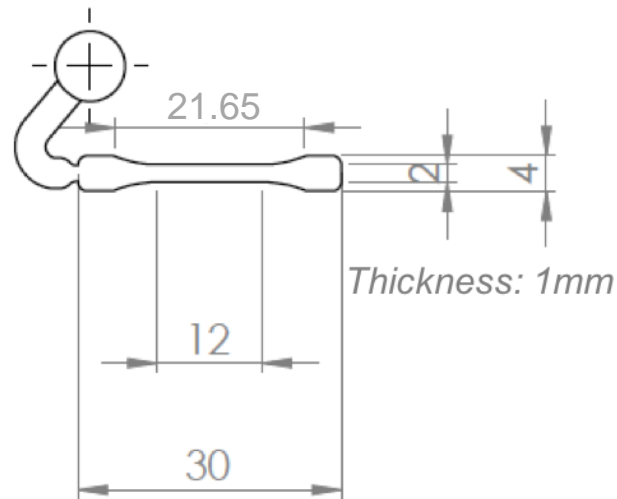


Figure 5. Tensile bar dimensions.

4.2. Materials

The materials presented in Table 3 were used: Polyamide 12 (PA12), polylactic acid (PLA) and nanoparticles of titanium dioxide (TiO_2).

For the elaboration of the test pieces with polyamide 12 (PA12), the necessary mass of material to fill the cavity mentioned in the previous section was calculated, using the volume of the cavity and the density of the material. It is necessary to consider that the riser

(in order to reduce material waste) must be less than 2 mm high [37]. The total mass necessary for filling the cavity was 0.27540 (g), which is equivalent to 17 pellets. The PA12 material before being used was dried at a temperature of 80 ° C for twelve hours. This was done, since the humidity of the environment affects during the molding process. When obtaining the dry material, it was weighed to obtain samples of approximately 0.27 g.

For the elaboration of the test tubes with polylactic acid (PLA), the total mass necessary for filling the cavity was 0.33480 g, which is equivalent to 8 pellets. PLA material before being used was dried at a temperature of 80°C for twelve hours. When obtaining the dry material, it was weighed to obtain samples of approximately 0.24 g.

Table 3. Properties of the materials.

	PA12	PLA	TiO₂
Name	Rilsamid™ PA 12 G AMNO TLD	Ingeo™ Biopolymer 3251D	Titanium (IV) oxide, rutile- nanopowder
Supplier	Arkema	NatureWorks	Sigma- Aldrich
Delivery form	Pellets	Pellets	Powder or Crystals
Density	1.02 g/cm ³	1.24 g/cm ³	-
Melt Temperature	260°C	188-210°C	-
Size	-	-	<_ 100 nm

5. Methodology to stabilize parameters in USM

The carried-out methodology is structured for each stage of the process. Within the six stages mentioned in the previous section, the Feeding and Cooling stages were not evaluated within the methodology. In each of them, the most relevant parameters (discussed in Table 2) must be identified, according to the expected outputs from each phase. The evaluated answers or outcomes were selected because in the Ultrasonic Molding Handbook [37], those that are relevant for having a successful stage in the process are mentioned. The outputs evaluated in the stages of the process are explained below (Table 4).

Table 4. Stages of the process with their outputs to evaluate.

Phases	Outputs
Compaction	Plunger Position
	Flat surface
Pre-heating	Cylinder Formation
	% Pellets Melted
Melting	% Filled Piece
Filling	% Filled Piece

1. Compaction.

- Plunger Position: This output is measured on the machine screen, where it indicates the initial position of the plunger and, once the process has been completed, it shows its final position. This is important because the higher the plunger gets; it means that there was better compaction of the material (**Figure 6. Examples of Compaction Outputs.**Figure 6).
- Flat surface: This output is evaluated visually, since you can see how compacted the pellets are. Compaction depends on the material that was used, as well as the size and shape of them (**Figure 6. Examples of Compaction Outputs.**Figure 6).

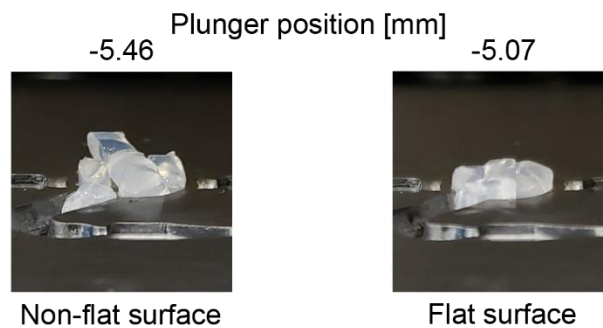


Figure 6. Examples of Compaction Outputs.

2. Pre-heating.

- Cylinder formation: It is relevant to observe if with the applied vibration, as well as the force, it allows a complete cylinder to be formed with all the pellets (Figure 7).

- % Pellets Melted: A measurement was performed depending on how many of the pellets had already been melted, forming the required cylinder (Figure 8).

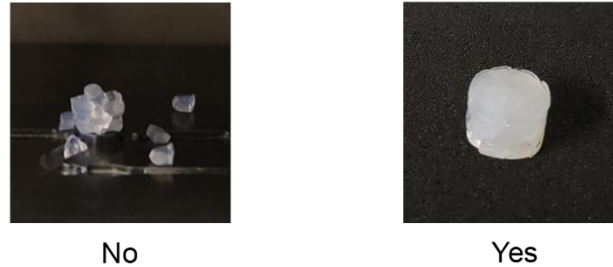


Figure 7. Example of Pre-heating Outputs (Cylinder Formation).



Figure 8. Examples of Pre-heating Outputs (Melted Pellets).

3. Melting.

- % Filled Piece: At this stage, it is important to observe what percentage of the part has been filled with the material. The more advancement in the filling means the better for the stage. To measure this output, the obtained piece was compared against a real-scale diagram of the piece with referenced marked percentages. These percentages were calculated with the surface area (Figure 9).



Figure 9. Examples of Melting Outputs.

4. Filling.

- % Filled Piece: It was measured in the same way as in the previous stage. However, the average of the cylinder filling percentages must be higher (Figure 10).
- Completed piece: This answer is binary and is expected to be yes, since it indicates that the objective was achieved.



Figure 10. Examples of Filling Outputs.

For the expected outputs (Figure 11), in the compaction phase, it is desired to see the plunger position as high as possible, as well as a flat surface, since this reduces the space between the pellets, and it allows more friction. For the Pre-heating phase, a 100%-cylinder formation is expected, and the pellets would be 80% melted. In the Melting phase, a percentage of filling of the specimen is expected between 40-60%. Lastly, in the Filling phase, 100% of specimen filling is expected to obtain a complete piece.

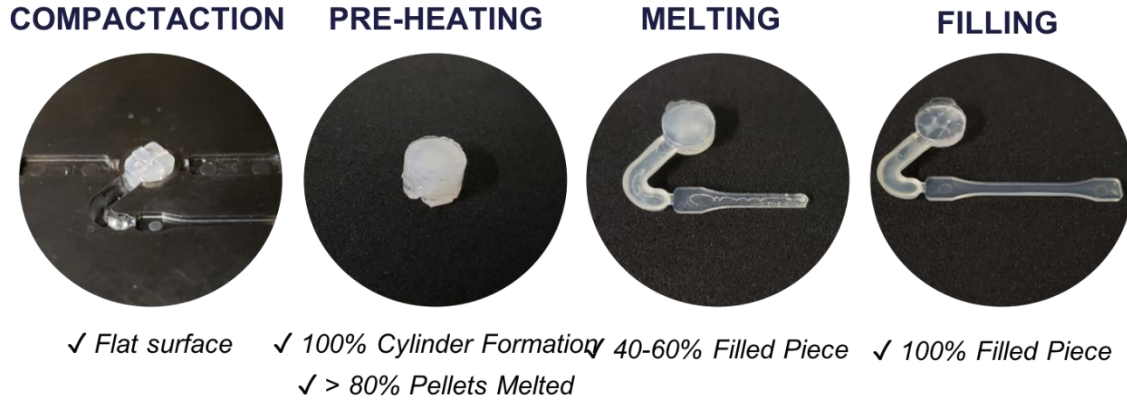


Figure 11. Examples of Expected Outputs.

6. Experimentation with neat material: PA12 y PLA.

The carried-out experimentation for the neat materials (PA12 and PLA) was developed in three phases: Preliminary experimentation, First experimentation and Final experimentation (Figure 12).

In the preliminary experimentation the proposed ranges for the parameters by the Ultrasonic Molding Handbook [37] depending on the material were considered, and different combinations were made in order to obtain a guide to elaborate an experimental design.

In the first experimentation, the design of experiments was carried out, based on preliminary experimentation and the ranges of the proposed values by the Ultrasonic Molding Handbook [37]. In this way, the methodology presented in the *Methodology to stabilize parameters in USM* section was carried out. For this, the outputs were validated by statistical analysis and finally, a first process parameters window is obtained. Each combination of parameters was performed 5 times.

The final experimentation was carried out in order to improve the repeatability of the process. Certain parameters are adjusted to improve expected outputs. The results are analyzed again with a statistical analysis and the final process parameters window is obtained.

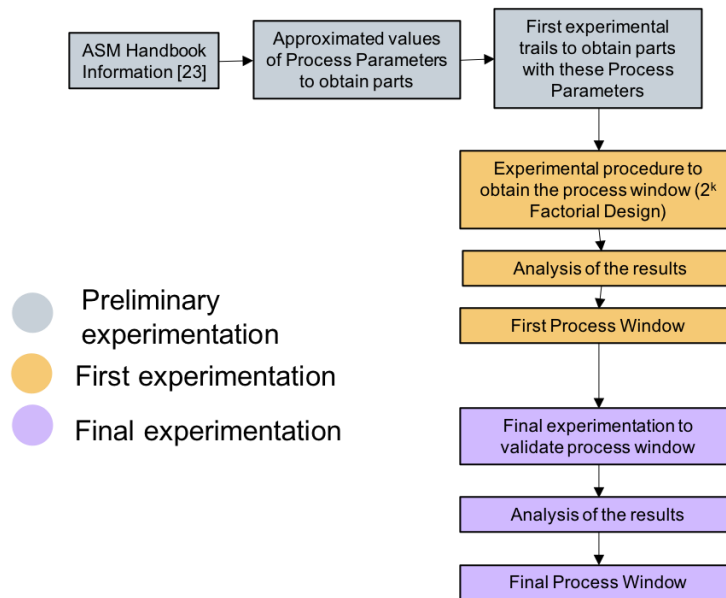


Figure 12. Experimental Procedure.

6.1. Preliminary Experimentation

In the preliminary experimentation phase, a previous experimentation was carried out to define parameters in order to obtain a process window. In this experimentation, the parameters recommended by the Ultrasonic Molding Handbook [37] were taken as a basis for each of the process steps, as well as for the materials used, and different combinations of them were made without repetition. Thus, in each of the stages of the process, those combinations were selected that would provide an expected result. If the material is not found in the Ultrasonic Molding Handbook, a material with similar properties is sought that is included in the Ultrasonic Molding Handbook [37] or in literature. For the definition of the parameters it is important to carry out each stage separately in order to obtain the correct values. The stages must be developed to start with Compaction, then Pre-heating, the Melting phase and finally Filling. Therefore, 0's are placed in time to cancel the stages that were already worked.

Compaction

For the Compaction phase, the velocity and force recommended by the Ultrasonic Molding Handbook [37] were left and only the number of strokes was defined. For the definition of strokes, three strokes were tested in a continuous way, in order to achieve a

change in the material. Two repetitions were performed for each strokes number test. Once the combinations were finished, the one with the highest average position of the plunger was selected.

Pre-heating

Once the strokes were defined, these parameters were maintained, and the Pre-heating stage was passed. The time was kept constant, while the amplitude and the force were varied. Those tests were selected where at least a 100% cylinder will be formed and the one with the highest percentage of melted pellets. By selecting amplitude and strength, other experiments were performed where time was varied. The outputs of 100% formed cylinder and the one with the highest percentage of melted pellets were selected and were considered again.

Melting

In the Melting stage, a travel depending on the material was calculated 2.1 mm and 2.2 mm for PA12 and PLA, respectively. The velocity was fixed at 0.5 mm / s, while the amplitude and force, recommended by Ultrasonic Molding Handbook [\[37\]](#), were varied. The combination with the highest percentage of cylinder filling was selected. Then the experimentation was carried out again, varying Velocity and Travel. The parameters that had the best percentage of test tube filling and where the Travel was the closest to the calculated were chosen.

Filling

Finally, in the Filling stage, experimentation was carried out by varying Force, Velocity and Time. According to the Ultrasonic Molding Handbook, it is recommended to start with a velocity of 1mm / s and a force of 2000 N and make increments of 500 N and use a time of 1 s. Those parameters that had a complete piece were chosen.

6.2. First Experimentation

Considering the results of previous experimentation, in this first experimentation a design of 2^k experiments was carried out, which is shown in Table 5. For each combination of parameters, 5 runs were made to obtain good reliability of the data.

Table 5. 2^k Factorial Design.

Phase	Parameters				Outputs	
		PA12		PLA		
Compaction	St	4	7	4	7	Plunger Position Flat surface
	A [%]	20	50	20	40	
Pre-heating	F [N]	200	300	200	400	Cylinder Formation % Pellets Melted
	T [s]	2	4.5	1	3	
	A [%]	40	60	40	50	
Melting	F [N]	650	850	500	625	% Filled Piece
	V [mm/s]	0.40	0.60	0.50	1.00	
	Tr [mm]	2.2		2.1		
	F [N]	2000	3000	2000	3000	
Filling	V [mm/s]	1	2	0.50	1.00	% Filled Piece
	T [s]	1	5	1	2	

The experimentation was carried out using the order of the methodology to evaluate the outputs at each stage. Once the experimentation was finished, a statistical analysis was performed to analyze the main effects, as well as the interactions of the parameters in each of the outputs. The full statistical analysis is found in detail in *Results and Discussion*.

6.3. Final Experimentation

After concluding the second stage of the first experimentation, it was decided to improve the repeatability of the process. For the PA12, when observing that not all the pieces came out complete and in the part of the riser, there was no more material that could be distributed, it was decided to analyze the variable of the number of pellets. Increased from 15 pellets to 17 and then to 18 pellets. On the other hand, when increasing the mass, the amplitude had to be increased in the Melting phase, to melt all the material introduced.

On the other hand, another of the varied parameters, for both materials was Travel, in the Melting phase. By setting this phase by Travel and not by time, the applied energy was not enough. The results are explained in the Results and Discussion section.

7. Experimentation with blends: PLA + TiO₂

7.1. Blends Preparation: Mixing, Milling and Sieving Process.

The mixture that was made was PLA with TiO₂ nanoparticles, using concentrations of 2.5, 5.0, and 7.5 wt. %.

For the preparation of the blends, PLA pellets, previously dried, were used in order to eliminate variables that affect the process. The equipment used was a Brabender 30/50 EHT mixer: Measurement and Control System. This mixer has the ability to process 50 g of material per batch. In this way, three batches were made for each of the mixtures, thus obtaining 150 g of each mixture. The conditions used for the mixture was a temperature of 190 °C at 80 rev / min and with a time of 10 minutes of processing. At the end of the processing time, the material is removed to collect it and move on to the next milling stage (Figure 13).

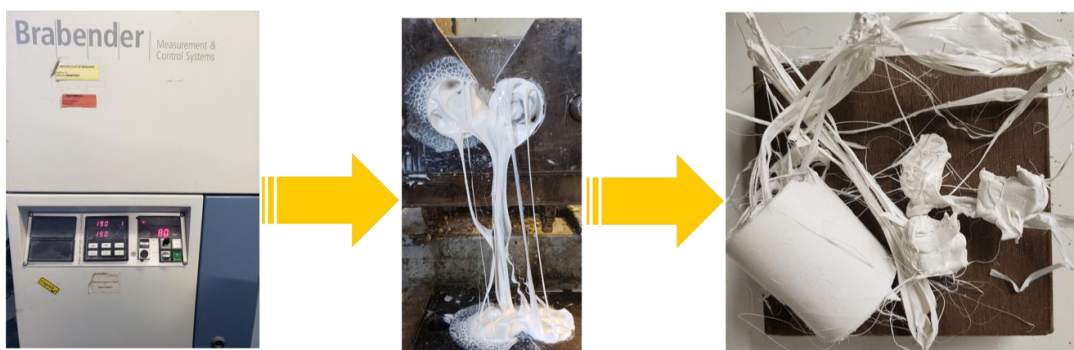


Figure 13. Mixing Process.

In order for the material to be used in ultrasound molding, it needs to be milled to obtain the material with a size smaller than 8 mm because the plasticizing chamber has this diameter. In addition, the material should be the same size on average to avoid clogging during molding. A Retsch SM 100 mill was used for crushing. The material is introduced and

pushed so that it passes into the cylinder which, through rotations, crushes the material (Figure 14).



Figure 14. Milling Process.

The sieves used were five that were manufactured with additive manufacturing in a 3D printer model BCN3D Sigma Release 2017. These sieves were created to carry out a previous work [39]. The design of each sieve is based on circular circular $\text{Ø}200$ mm and height 0.8 mm. According to Ariadna's work [39], the particle sizes <3.8 mm and <4.5 mm work for this process. However, in this work, <4.5 mm was used as they worked properly (Figure 15).

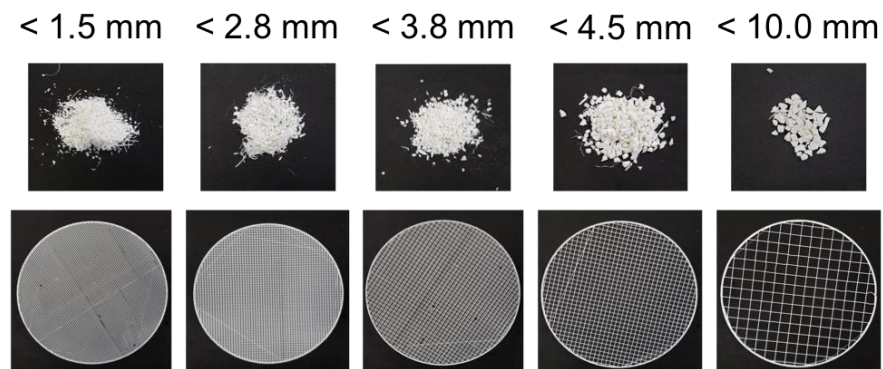


Figure 15. Sieving Process.

7.2. Experimental Procedure with Blends: PLA + TiO_2

For the experimentation of blends, the parameters obtained for the neat PLA (Process Parameters Window) were taken as a base, taking this window, three repetitions

were made for each blend. The outputs were evaluated, and the final process parameters window for the blends was obtained. It is worth mentioning that there was no change regarding the window of the neat PLA. 20 pieces were made with the final process window for each mixture to characterize them.

7.3. Parts Characterization Conditions.

The manufactured parts were characterized in order to obtain morphological (SEM), physical-chemical (MFI, XRD, FTIR), and mechanical (Tensile testing) properties to observe the influence of the ultrasonic molding process on the material and the behavior by increasing the concentration of nanoparticles.

7.3.1. Scanning Electron Microscopy (SEM).

The Scanning Electron Microscopy (SEM) technique was performed with the objective of analyzing the topography of the material, as well as observing the distribution and integration of the nanoparticles depending on the concentration.

The samples were cleaned with distilled water with isopropanol (1:1) in the Branson 2800 equipment (Figure 16) with an ultrasound time of 5 minutes. Subsequently, a cross section was made to the samples and they were placed on an aluminum pin-stub using a double-sided adhesive carbon tape. The samples were covered with a thin layer of gold using Quorum Q150R - Rotary Pumped Coater (Figure 17).



Figure 16. Branson 2800 equipment.



Figure 17. Quorum Q150R – Rotary Pumped Coater.

The technique was performed using a Zeiss EVO-MA25 microscope (Figure 18) operating at 5kV and high vacuum. The characterized pieces were manufactured under optimal conditions chosen (Process Parameters Window). The images were made at different magnifications: 2000, 1000 and 200 X.

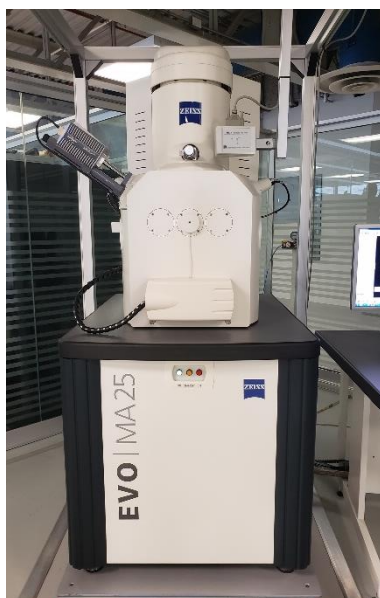


Figure 18. Zeiss EVO-MA25 microscope.

7.3.2. Melt Flow Index (MFI).

The objective of this technique was to know the fluidity of the polymer and how it changed with the increase in TiO₂ nanoparticles. It is also an indirect measure of molecular weight: High melt index values, low molecular weight, and low values mean high molecular weight. The technique was performed four times for each type of sample. 2.25 g of material

was taken for each test with a temperature of 210°C by using Ceast-Melt Flow Quick Index (Figure 19). At the end, an average was made for each set of sample type. Outputs were measured in g/10 min.



Figure 19. Ceast – Melt Flow Quick Index

7.3.3. X-Ray Diffraction (XRD).

X-ray diffraction allows analysis of whether the mentioned materials are being used, as well as observing the crystal structures in which the materials are found.

XRD patterns of the different types of materials were prepared using an X-Ray diffractometer (Panalytical Empyrean) (Figure 20) equipped with Cu radiation at a wavelength of 1.5406 Å. Measurements were obtained with a scanning rate of 0.95°/s and a diffraction angle range of 10 to 85° (2-Theta° range) at room temperature.



Figure 20. Panalytical Empyrean.

7.3.4. Fourier-Transform Infrared Spectroscopy (FTIR).

The FTIR analysis was carried out with the objective of analyzing the chemical composition (Functional Groups) of the samples, as well as the interaction of the materials depending on the composition (Concentration). Also, through this analysis the influence of the process on the different parts of the piece made is observed and if degradation occurred.

FTIR spectra were collected for neat PLA and PLA with TiO₂ in all the different concentrations (2.5, 5.0 and 7.5%) using a PerkingElmer FT-IR / FIR Spectrometer (Figure 21). Each sample was scanned 16 times between 4000 and 400 cm⁻¹, with a resolution of 4 cm⁻¹ at room temperature.



Figure 21. PerkingElmer FT-IR / FIR Spectrometer.

7.3.5. Tensile Testing

The technique was performed to observe the resistance to break that TiO₂ nanoparticles can add to the PLA. In addition, to analyze the influence of the ultrasonic molding process on the mechanical properties.

The mechanical properties of the samples were determined using the Instron 3365 Universal Testing Machine (Figure 22) with a load cell of 5kN capacities. The measurements were made with a velocity of 5 mm / min and 5 samples were measured for each material (PLA, PLA + 2.5% TiO₂, PLA + 5.0% TiO₂ and PLA + 7.5% TiO₂).



Figure 22. Instron 3365 Universal Testing Machine.

8. Results and Discussion

8.1. Analysis of the Experimental Results

After having carried out the experimentation to analyze the influence of the parameters on each of the outputs corresponding to each phase of the process, a statistical analysis was performed in Minitab. The different combinations of parameters were analyzed with an analysis of variance to obtain those parameters or interactions of them that were significant. Due to the variability of the process, a 90% confidence level was proposed.

8.1.1. Results in First Experimentation

When performing the statistical analysis, for each phase the parameters that were significant were obtained, depending on the output that was analyzed in each of them. The significant parameters are shown in Table 6 for PA12 and in Table 7 for PLA. For the conclusions, it is not only taken into account if the parameter is significant. The means and standard deviations are considered to analyze the stabilization of the process.

Table 6. Significant Parameters for PA12.

Phases	Parameters	Outputs	Significant Parameters (p-value)
Compaction	St	Plunger Position	-
		Flat surface	-
Pre-heating	A [%] F [N] T [s]	Cylinder Formation	A – 0.000 T – 0.067 A*T – 0.067
		% Pellets Melted	A – 0.000 F – 0.000 T – 0.000 All the interactions
Melting	A [%] F [N] V [mm/s] Tr [mm]	% Filled Piece	F – 0.087
Filling	F [N] V [mm/s] T [s]	% Filled Piece	-

Table 7. Significant Parameters for PLA.

Phases	Parameters	Outputs	Significant Parameters (p-value)
Compaction	St	Plunger Position	St – 0.010
		Flat surface	-
Pre-heating	A [%] F [N] T [s]	Cylinder Formation	A – 0.000 F – 0.000 T – 0.030 All the interactions
		% Pellets Melted	A – 0.000 F – 0.001 A*F – 0.000
Melting	A [%] F [N] V [mm/s] Tr [mm]	% Filled Piece	A – 0.000 F – 0.058 A*F – 0.094 F*V – 0.003
Filling	F [N] V [mm/s] T [s]	% Filled Piece	F – 0.058

Compaction

In the Compaction stage, there is only one parameter that varies; therefore, the output depends 100% on it. According to the results obtained for both materials, the greater the number of strokes, the higher the average plunger position, which indicates greater compaction. Although strokes are only significant for the PLA. However, the standard deviation represents stability in the outputs obtained and this depends on the nature and shape of the material's pellets. As shown in Figure 23 a), for PA12, 7 strokes coincide at the largest plunger position and have the least deviation. However, for PLA, 7 strokes have the highest plunger position but not the smallest standard deviation. For PA12, 7 strokes were selected and for PLA, 5 strokes.

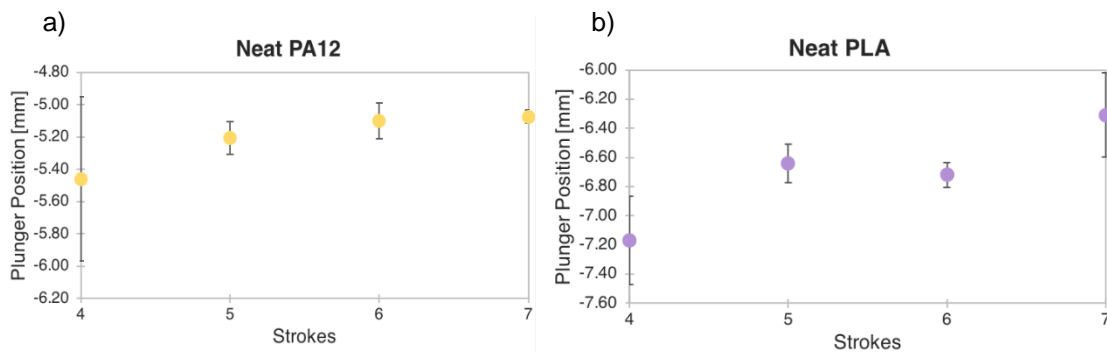


Figure 23. Output in Compaction, a) Plunger Position for PA12 and b) Plunger Position for PLA.

Pre-heating

In the Pre-heating stage, it was identified that the three parameters, Amplitude, Force and Time, are significantly involved in the expected outputs for the two materials (Table 6 and Table 7).

Figure 24 shows the comparison of the combination of the lowest values for the parameters with the combination of the highest values for each output: Cylinder Formation and % Pellets Melted, for each material.

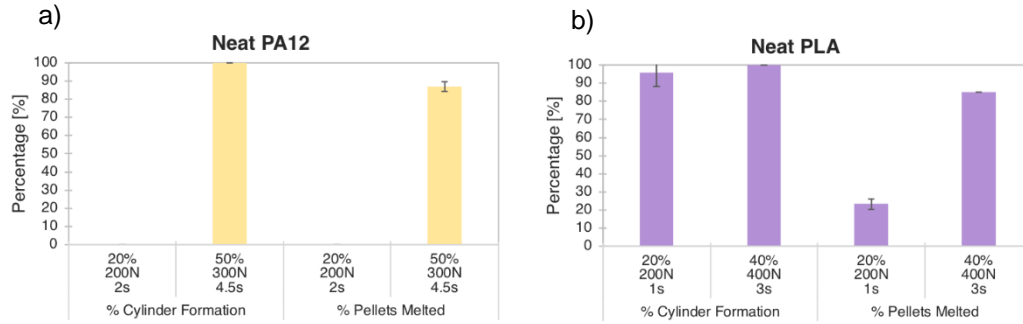


Figure 24. Outputs in Pre-heating, a) Outputs for PA12 and b) Outputs for PLA.

For both PA12 and PLA, the combination of the higher parameters gives the expected answers: 100% cylinder formation and over 80% of the melted pellets.

Melting

In the Melting phase, as seen in Figure 25, the combination of the larger parameters provides a higher percentage of filling of the cylinder. However, for PA12 only strength is significant. Therefore, force majeure must be used. However, since the amplitude and velocity are not significant, the most appropriate ones were used for the process. A smaller amplitude, less energy, less material degradation and at a higher velocity, less time in the process.

On the other hand, for PLA Amplitude and Strength are significant. So, the combination of the larger parameters was considered since its standard deviation shows greater stability, compared to PA12.

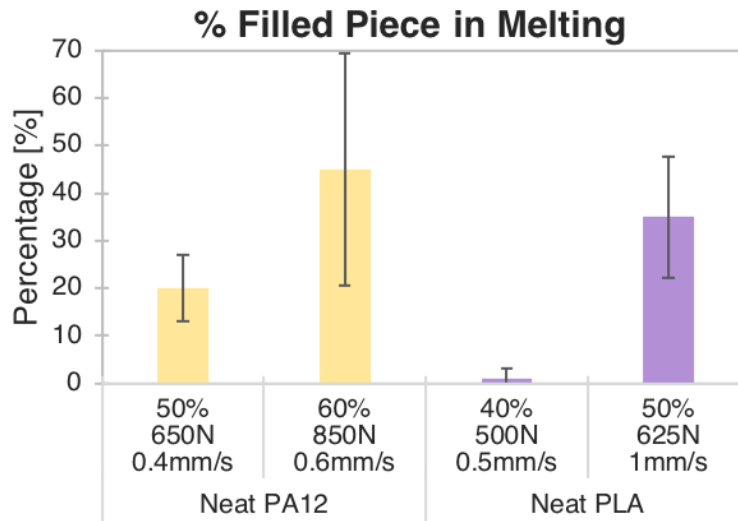


Figure 25. Outputs in Melting.

Filling

Lastly, in the Filling stage, for a higher specimen filling, a significant parameter was not found for PA12 and the Force is significant for PLA. As shown in Figure 26, for PA12, the combination of smaller parameters demonstrates a higher percentage of specimen. While for PLA, the combination of larger parameters has a higher percentage of cylinder filling. Due to the lack of significant parameters, the process shows more variability (greater standard deviation) in the expected outputs.

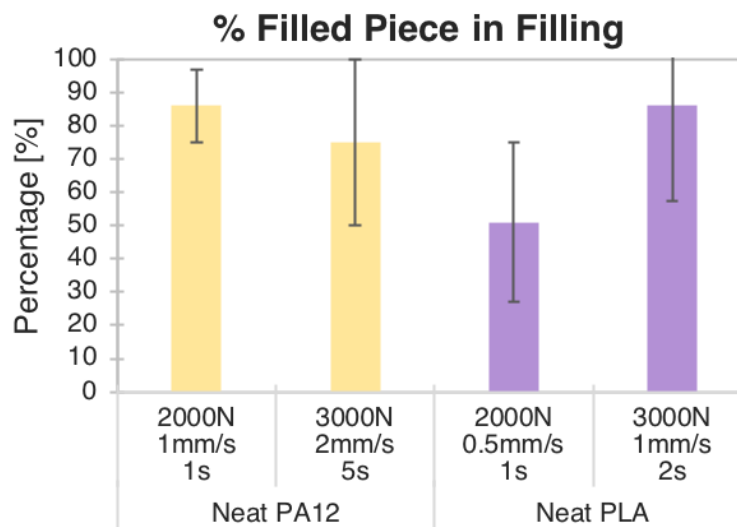


Figure 26. Outputs in Filling.

In conclusion, if the first three stages (Compactation, Pre-heating and Melting) have a good selection of parameters, the Filling stage can have a range of working parameters and in this way, those that suit the process are selected, taking into account the material and the process.

Table 8 and Table 9 show the first process parameters windows PA12 and PLA, respectively.

Table 8. First Process Parameters Window for PA12.

	A [%]	F [N]	V [mm/s]	T [s]	Tr [mm]	St	Pellets
Compactation	-	4000	10	-	-	7	15
Pre heating	0.50	300	-	4.5	-	-	
Melting	0.50	850	0.60	-	2.2	-	
Filling	-	2000	1	1	-	-	
Cooling	-	-	-	5	-	-	

Table 9. First Process Parameters Window for PLA.

	A [%]	F [N]	V [mm/s]	T [s]	Tr [mm]	St	Pellets
Compactation	-	4000	10	-	-	5	8
Pre heating	0.40	400	-	3	-	-	
Melting	0.50	625	1	-	2.1	-	
Filling	-	3000	1	2	-	-	
Cooling	-	-	-	5	-	-	

8.1.2. Results in Final Experimentation

In the final experimentation, adjustments were made to certain parameters in order to improve the repeatability of the process.

For PA12, the influence of the number of pellets used was analyzed. When performing the analysis, this variable was significant. As shown in Figure 27, the greater the number of pellets, the less the standard deviation, the greater the stability of the results. With 17 and 18 pellets, there is not much difference between the standard deviation, the average percentage of the cylinder filling is 4% higher with 18 pellets. With 18 pellets, the parameters of the Filling phase were changed, using the combination of the larger parameters.

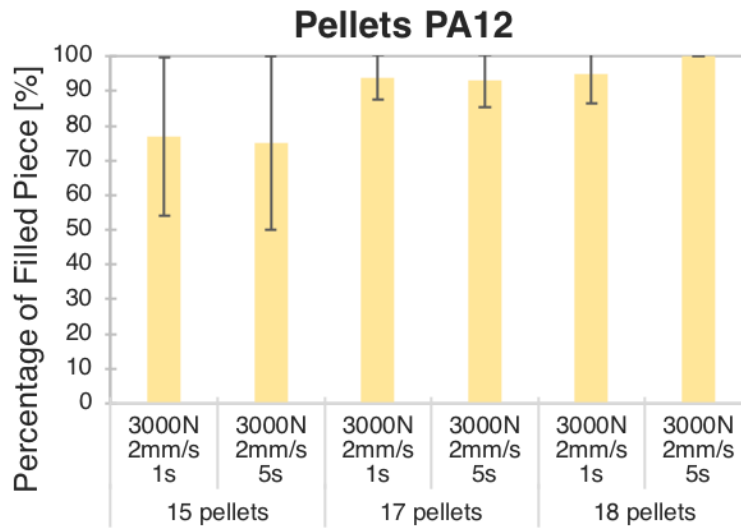


Figure 27. Influence of the pellets.

On the other hand, due to the increase in the pellets used, it was necessary to increase the amplitude in the Melting phase, in order to fuse all the material (Figure 28). Because of this, there was a significant change where with the amplitude of 0.6 in Melting and 18 Pellets, the % of filling of the cylinder rises by 17%. In addition, the standard deviation decreased.

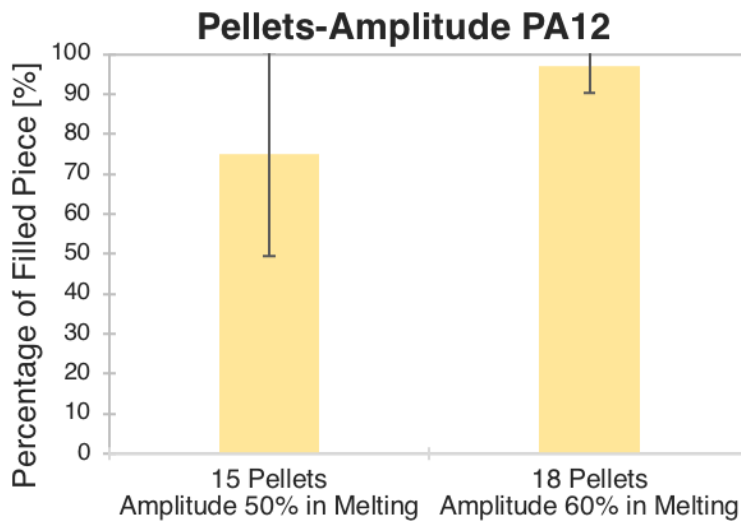


Figure 28. Pellets / Amplitude in Melting.

Finally, a change was made in the travel used in the Melting phase for both materials. This phase, when establishing a travel, the process established a random time for the

Melting phase. When performing the analysis, removing the travel (Travel = 0) and proposing a longer and more specific time for this phase, the percentage of filling of the test piece, and the repeatability of the process, increased (Figure 29). For PA12, it went from 60% to 80% of filled specimens, while for PLA, it went from 50% to 90% of filled specimens.

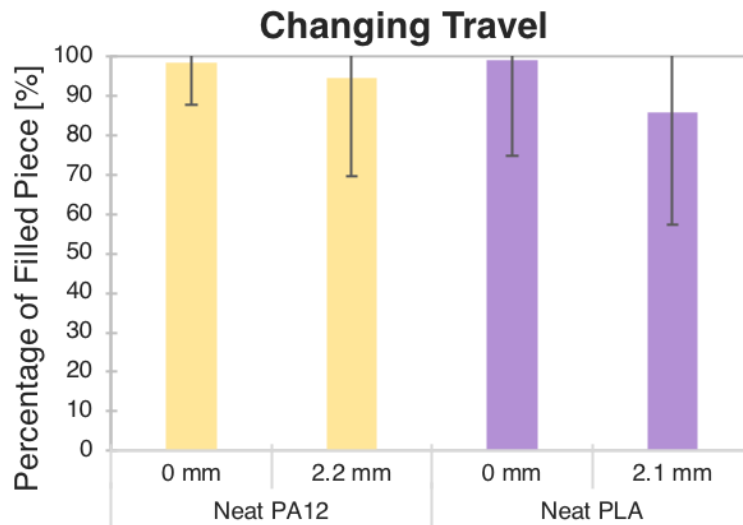


Figure 29. Travel Change.

Table 10 shows the comparison of the importance of the change of travel in the process taking as reference random pieces of PLA. When the travel was 2.1mm, the process stopped for time in the melting phase, which was approximately 0.70 s and was not a fixed time. This indicated that, for greater repeatability of complete parts, the melting phase should be carried out in a time greater than 0.70 s. Therefore, the travel was removed, and it was established that the process would be carried out by time and would be 1.3 s. Thanks to this, the repeatability of complete parts was improved. Increasing the time in the melting phase guarantees that the applied ultrasound energy will be greater. Therefore, it will help melt the material and allow filling.

According to the analysis performed, it was observed that the total applied ultrasound energy affects the percentage of filled piece. In this case must be greater than 260J (Figure 30) to obtain a complete piece for the PLA material. On the other hand, it is important to mention that it must be a combination with the mass used to fill the cavity.

Table 10. Travel Change Comparison.

Travel [mm]	Weight [g]	Filled Piece [%]	Melting Time (s)	Pre-heating Energy [J]	Melting Energy [J]	Total Energy [J]
2.1	0.329	95	0.58	156.130	101.054	257.184
	0.345	100	0.78	154.010	150.842	304.852
	0.341	100	0.68	152.800	107.016	259.816
	0.354	100	0.78	152.260	134.515	286.775
	0.334	35	0.63	128.230	107.247	235.477
0.0	0.353	100	1.29	116.464	242.847	359.311
	0.359	100	1.29	110.531	253.204	363.735
	0.350	100	1.29	142.103	260.913	403.016
	0.345	90	1.30	96.868	188.922	285.790
	0.335	100	1.29	130.266	259.817	390.083

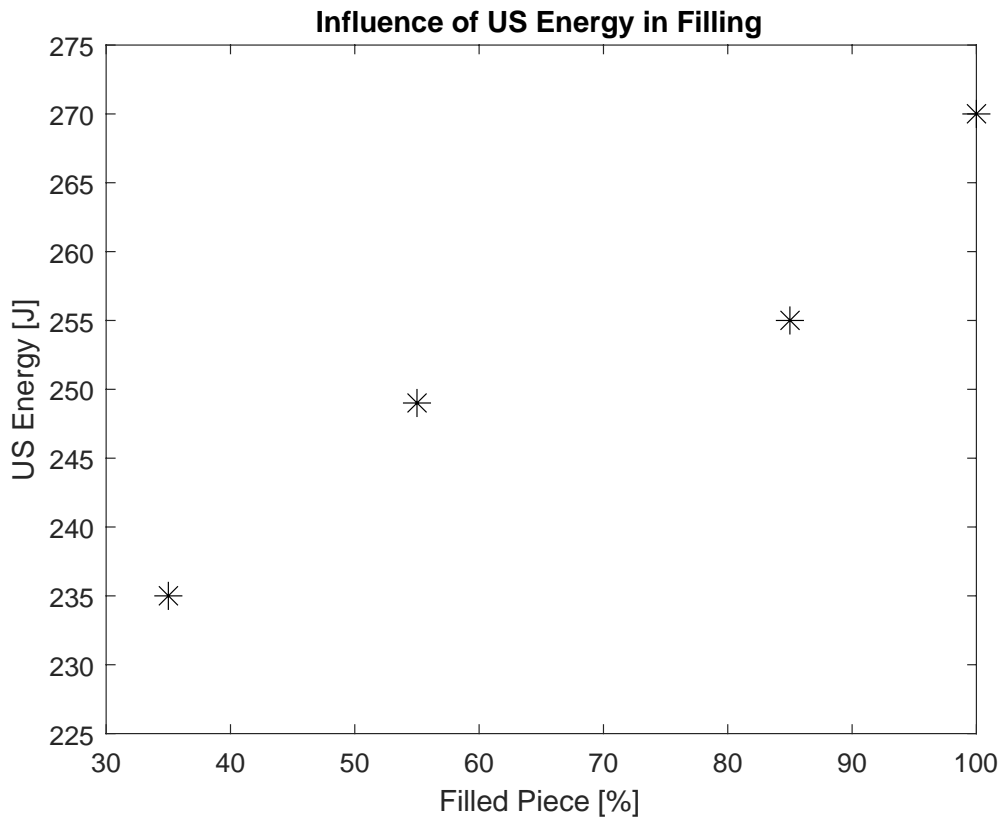


Figure 30. Comparison of US Energy vs % Filled Piece.

Finally, after these last changes, the final windows of process parameters for PA12, PLA and PLA / TiO₂ were obtained in Table 11, Table 12 and Table 13, respectively. It should be mentioned that there was no change in the window of the virgin PLA with that of the mixtures.

Table 11. Final Process Parameters Window for PA12.

	A [%]	F [N]	V [mm/s]	T [s]	Tr [mm]	St	Pellets
Compaction	-	4000	10	-	-	7	
Pre heating	0.50	300	-	4.5	-	-	
Melting	0.60	850	0.60	0.5	-	-	18
Filling	-	3000	2	5	-	-	
Cooling	-	-	-	5	-	-	

Table 12. Final Process Parameters Window for PLA.

	A [%]	F [N]	V [mm/s]	T [s]	Tr [mm]	St	Pellets
Compaction	-	4000	10	-	-	5	
Pre heating	0.40	400	-	3	-	-	
Melting	0.50	625	1	1.3	-	-	8
Filling	-	3000	1	2	-	-	
Cooling	-	-	-	5	-	-	

Table 13. Final Process Parameters Window for PLA/TiO₂.

	A [%]	F [N]	V [mm/s]	T [s]	Tr [mm]	St	Pellets
Compaction	-	4000	10	-	-	5	
Pre heating	0.40	400	-	3	-	-	
Melting	0.50	625	1	1.3	-	-	8
Filling	-	3000	1	2	-	-	
Cooling	-	-	-	5	-	-	

8.2. Parts Characterization

8.2.1. Scanning Electron Microscope (SEM)

Figure 31 shows that the mixtures contain agglomerates. For the images with a concentration of 2.5 wt. %, a cluster of approximately 10 μm in diameter is observed. On the other hand, the images with a concentration of 5 wt. %, an agglomerate of 6 μm in diameter is observed. However, for the concentration of 7.5 wt. % no clusters are observed. This behavior is unusual, because in different experiments carried out [40] as the concentration of nanoparticles increases, the dispersibility decreases and the agglomerates are induced to increase. This behavior may be due to the fact that in this experiment ultrasound is used

for the fusion of the material and a recommended process for the dispersion of nanoparticles is by means of ultrasound [36]. To more nanoparticles, the process is in charge of distributing them better in the Melting phase. However, more images must be taken to ensure this behavior.

On the other hand, as observed, the surface roughness increased with the increase of TiO₂ nanoparticles. The same behavior was observed in the experiment carried out by Feng et al. [40], they found that as nanoparticles increase, the texture of the material changes. This behavior may be since the material is more rigid with the increase in nanoparticles, however, it cannot be guaranteed, until confirmed with the tensile test.

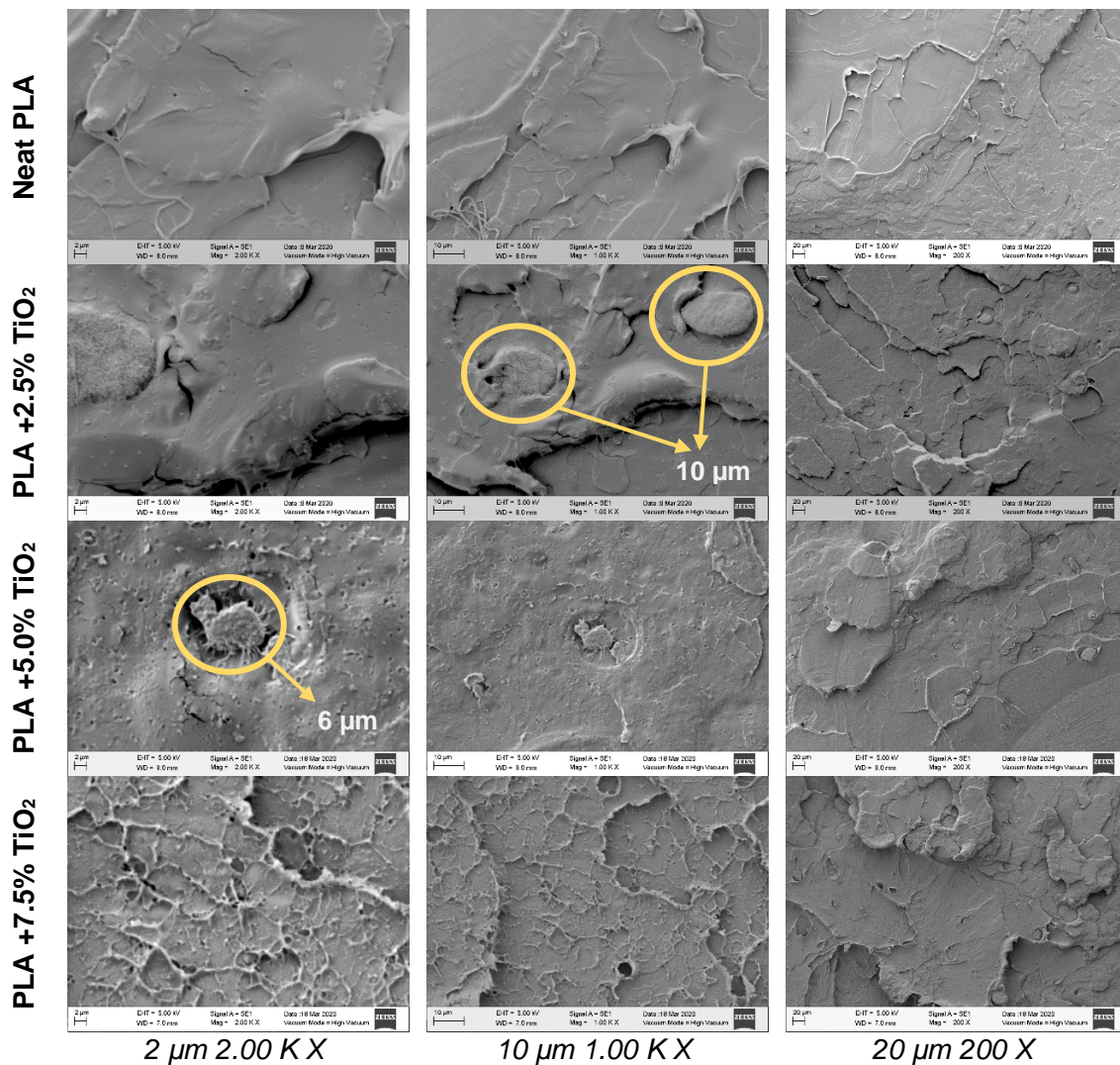


Figure 31. SEM Images of PLA/TiO₂ nanoparticles.

8.2.2. Melt Flow Index (MFI)

The results obtained are shown in Table 14.

Table 14. Melt Flow Index.

Material	MFI (g/10min)
PLA	74.44
PLA + 2.5%	83.86
PLA + 5.0%	96.76
PLA + 7.5%	104.49

According to Figure 32., it is observed that as TiO₂ nanoparticles are added to the PLA, the flow rate increases. This may be possible due to two causes: The observed behavior in SEM or the molecular weight. Regarding the behavior observed in SEM, the agglomerates decreased as the concentration increased and this can help the material flow more easily. On the other hand, with respect to the measurement of molecular weight, it could mean that the molecular weight decreases since the titanium dioxide nanoparticles interrupt the PLA chains and increase the space of the molecular chain [\[41\]](#). However, the decrease in molecular weight should be verified with the gel permeation chromatography (GPC) test to obtain an accurate conclusion.

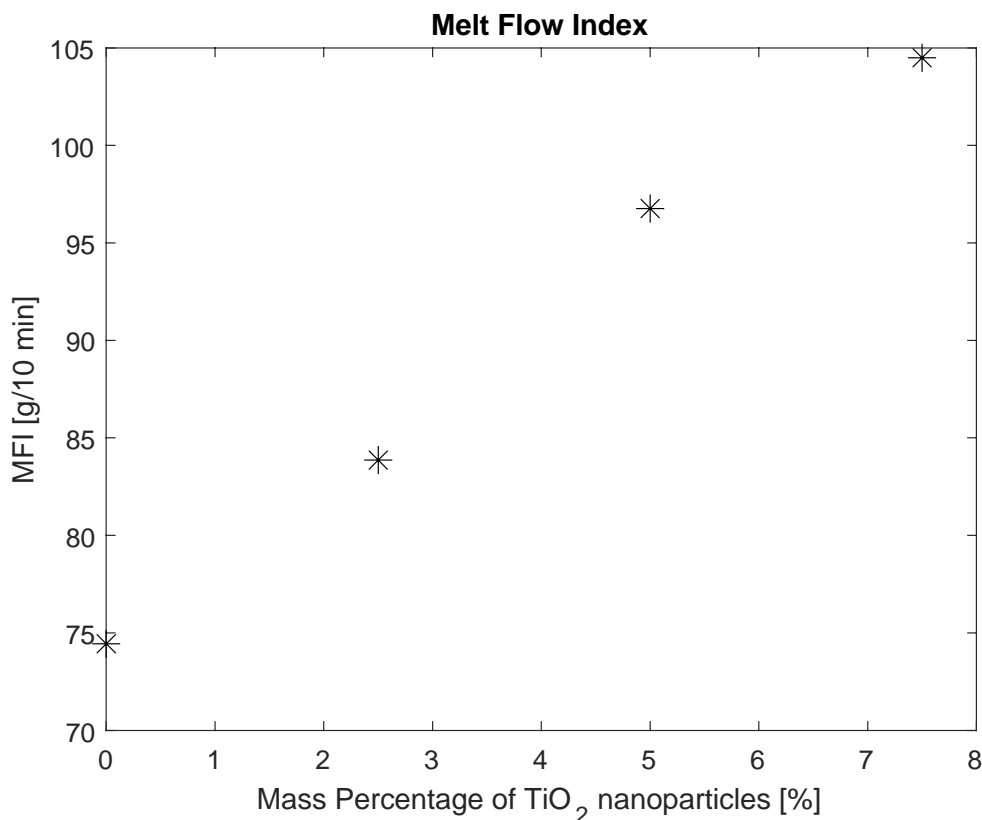


Figure 32. MFI with the increment of nanoparticles.

8.2.3. X-Ray Diffraction XRD

The X-ray diffractograms of the samples (Figure 33.) showed for the neat PLA, the hump located at $2\theta = 16$ indicating the amorphous nature of the material [41]. On the other hand, by analyzing the X-ray diffractogram for the blends, representative peaks for TiO₂ are added. These peaks increase in intensity, as the concentration increases. Because TiO₂ is a polymorphic material, it means that it can be found in different phases, including: Rutile and Anatase. For the rutile phase, the XRD peak at 24.61 represents (1 1 0) crystal plane. On the other hand, the XRD peaks at 47.41, 53.32 and 54.45 correspond to anatase (2 0 0), (1 0 5) and (2 1 1) crystal plans [42][43]. According to the technical data sheet of the material indicates that the particles are in rutile phase with 5-10% anatase. When performing, this diffractogram reflects a rutile / anatase combination, since TiO₂ that is in the anatase phase was not converted to rutile due to the energy used in the process. According to Zhang et al. [44] found that the start of the crystalline anatase phase is around 210°C and the anatase-rutile transition is reported to occur between 400 and 1000°C [45]. Because of

the process, these temperatures are not being reached and that is why the combination of phases. In conclusion, the XRD patterns demonstrate that the PLA structure is not affected by the presence of TiO₂ nanoparticles [42].

Table 15 shows the comparison of the peaks for both phases with the peaks obtained in the diffractograms.

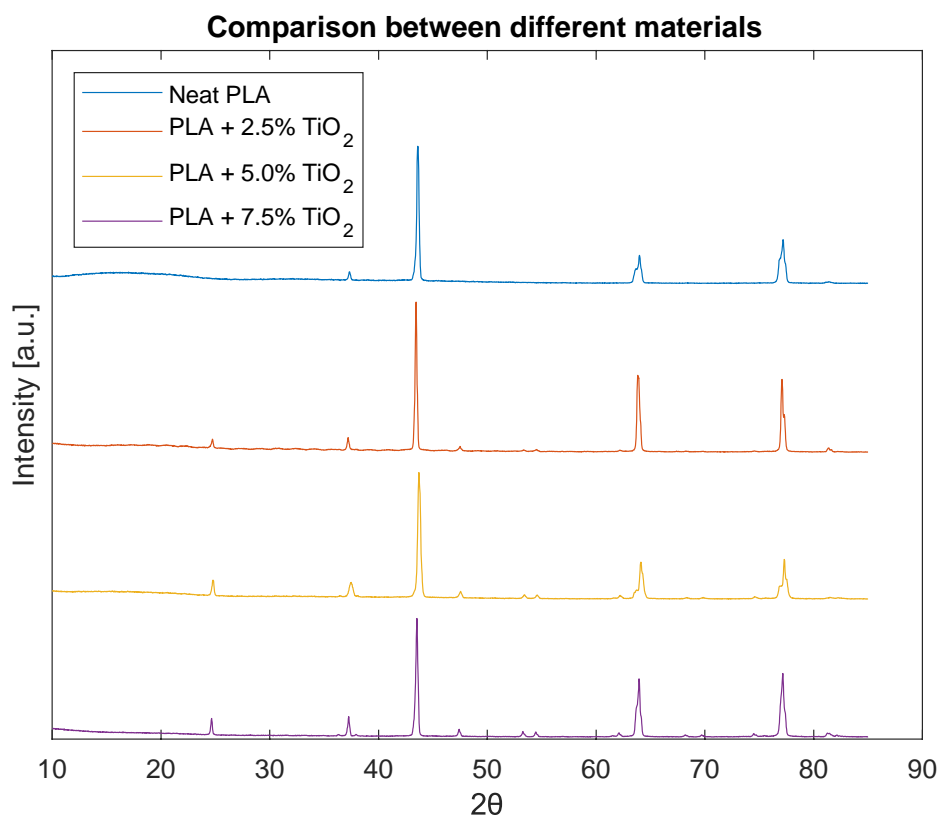


Figure 33. XRD - Comparison between the different materials.

Table 15. Both phases for TiO₂: Rutile and Anatase.

2θ	2θ Rutile (hkl)	2θ Anatase (hkl)
24.61	27.4 (1 1 0)	25.3 (1 0 1)
47.41	41.2 (1 1 1)	48.0 (2 0 0)
53.32	54.3 (2 1 1)	53.9 (1 0 5)
54.45	56.6 (2 2 0)	55.0 (2 1 1)

8.2.4. Fourier-Transform Infrared Spectroscopy (FTIR)

Two points of the piece were observed: at injection point and at the center (Figure 34.).

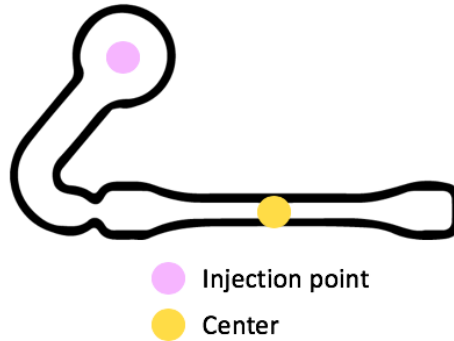


Figure 34. Points of analysis.

With Figure 35, the comparison between the two points of the part is shown. There is a difference in transmittance between them, because at the injection point, there are pellets that were not melted and prevent the passage of energy. Thanks to this, the homogeneity of the material can be observed (Figure 36.). It is important to note that for this process, the FTIR should not be performed at the injection point, since the reflected transmittance makes it difficult to interpret the results due to the lack of homogeneity.

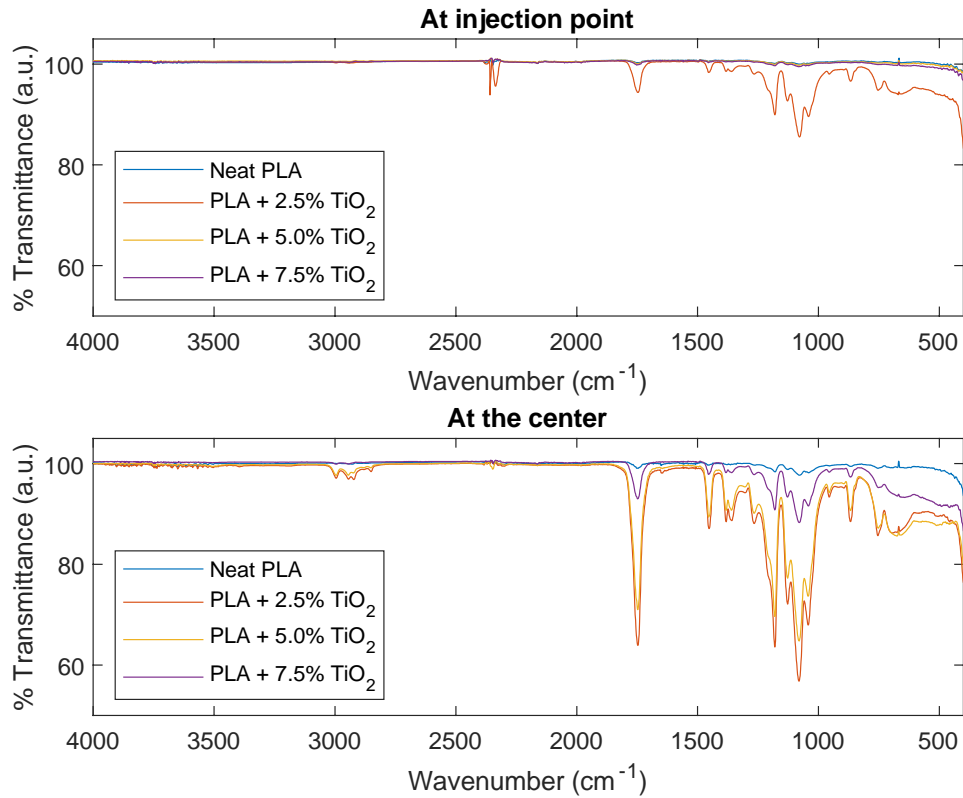


Figure 35. FTIR Spectra – Comparison between different analysis points.

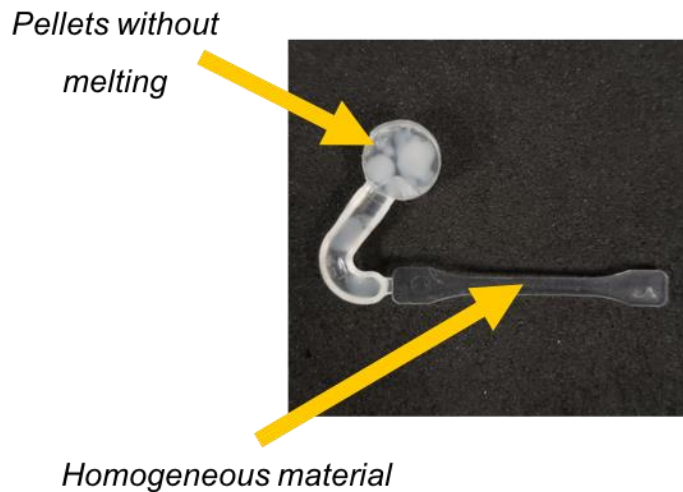


Figure 36. Homogeneity difference between the two points analyzed.

In Figure 37, the spectra for the neat PLA and for the PLA/TiO₂ blends are shown. The PLA spectrum showed the weakest peak at 1751 cm⁻¹ that is due to stretching carbonyl vibration C = O [46][47][48]. Another transmittance peak at 1179 cm⁻¹ is due to formate

stretching vibration [46] and the last peak at 1079 cm^{-1} due to stretching vibrations of C-O-C bonds [46]. In the spectrum of PLA / TiO_2 , the 2923 cm^{-1} peak represents the stretching vibrations of $-\text{CH}_3$ and $-\text{CH}_2$ of neat PLA. On the other hand, this band due to its location may represent the hydroxyl group, since TiO_2 is polar and can attract humidity from the environment. The peaks at 1381 cm^{-1} and 1179 cm^{-1} are due to carboxyl stretching vibration and formate stretching vibrations respectively [46].

The addition of nanoparticles keeps the signal of 1749 cm^{-1} (Carbonyl Stretching) and 1082 cm^{-1} (C-O-C) unchanged, which could be due to a physical mixture between the components. However, the intensity of the peaks increases in PLA / TiO_2 compared to neat PLA. Similar results occur in the experimentations reported by Feng et al. and Li et al. [40][49]. Finally, the characteristic band representing TiO_2 is located at 751 cm^{-1} , due to the Ti-O-Ti bonds [47].

As can be seen (Figure 37), at a lower concentration of nanoparticles, the transmittance of the bands is higher, due to the opacity that TiO_2 brings to the material. Feng et al. [40] report that the less TiO_2 nanoparticles, the greater the energy transmitted in the material. In general, the interaction between the materials is physical, because no new bands are observed [40]. On the other hand, there was no degradation of the materials, since no band disappeared from the spectrum.

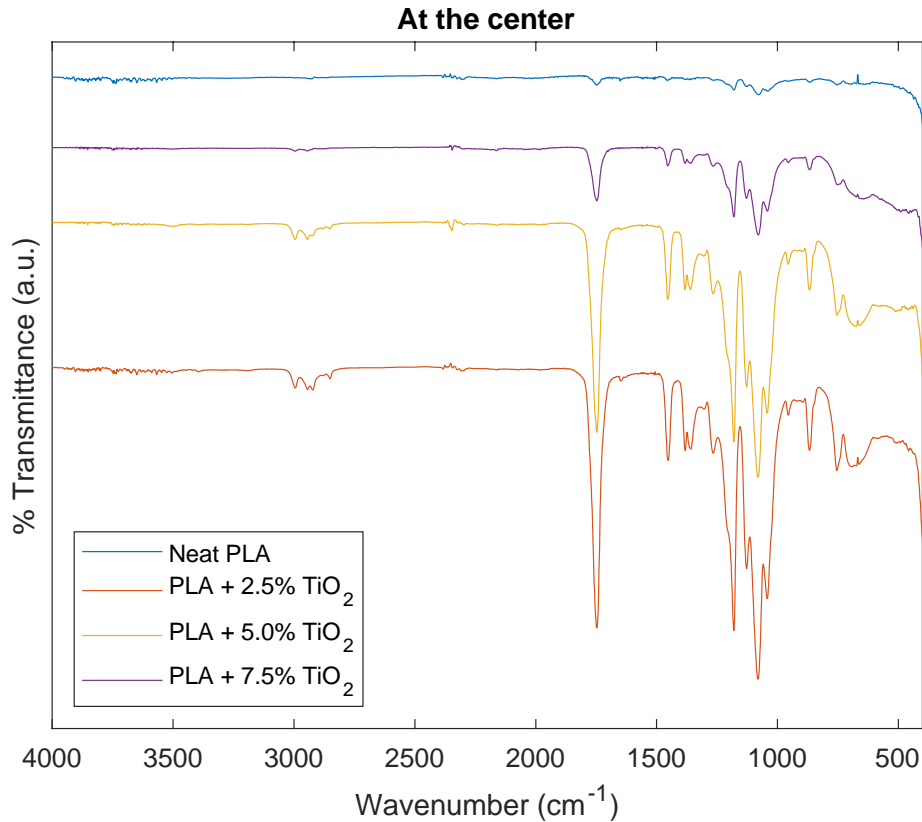


Figure 37. FTIR Spectra – Comparison between different materials at the center.

8.2.5. Tensile Test

In the Table 16, the mechanical properties obtained for the neat PLA and the different concentrations of TiO_2 are shown. They are represented through average data and standard deviations. In addition, Figure 38. shows the graph for the behavior of different materials.

As can be seen, Young's modulus (E) increases at a higher concentration of nanoparticles, which indicates that the material is stiffer as observed in the SEM results. Young's modulus increased from 3724.2 MPa with neat PLA to 3956.7 MPa for the concentration of 7.5 wt. %, that is, an increase of 6.24% with respect to neat PLA. This is due to the crystallization that TiO_2 provides [40]. In addition, when observing the standard deviation for Young's modulus, it decreased with increasing nanoparticles, which indicates stability since they reach the point of distributing the nanoparticles throughout the piece and possibly, due to the reduction of agglomerates. Comparing neat PLA with PLA / TiO_2 , the piece showed higher tensile strength and elongation at break. The tensile strength may be

due to the creation of the crystal structure due to nanoparticles [40]. On the other hand, a trend is not observed as nanoparticles are added. This varies depending on the agglomerates that may exist in the pieces [50].

Table 16. Tensile Testing Analysis.

Material	US Energy[J] (SD)	E [MPa] (SD)	σ_u [MPa] (SD)	ϵ_t [%] (SD)
Neat PLA	368.7 (± 29.3)	3724.2 (± 135.5)	52.65 (± 8.09)	0.018 (± 0.007)
PLA + 2.5 % TiO ₂	313.9 (± 40.9)	3787.7 (± 74.6)	56.88 (± 4.59)	0.019 (± 0.006)
PLA + 5.0 % TiO ₂	313.7 (± 32.8)	3811.8 (± 71.0)	53.63 (± 9.14)	0.019 (± 0.007)
PLA + 7.5 % TiO ₂	276.7 (± 37.6)	3956.7 (± 42.9)	57.60 (± 5.72)	0.023 (± 0.008)

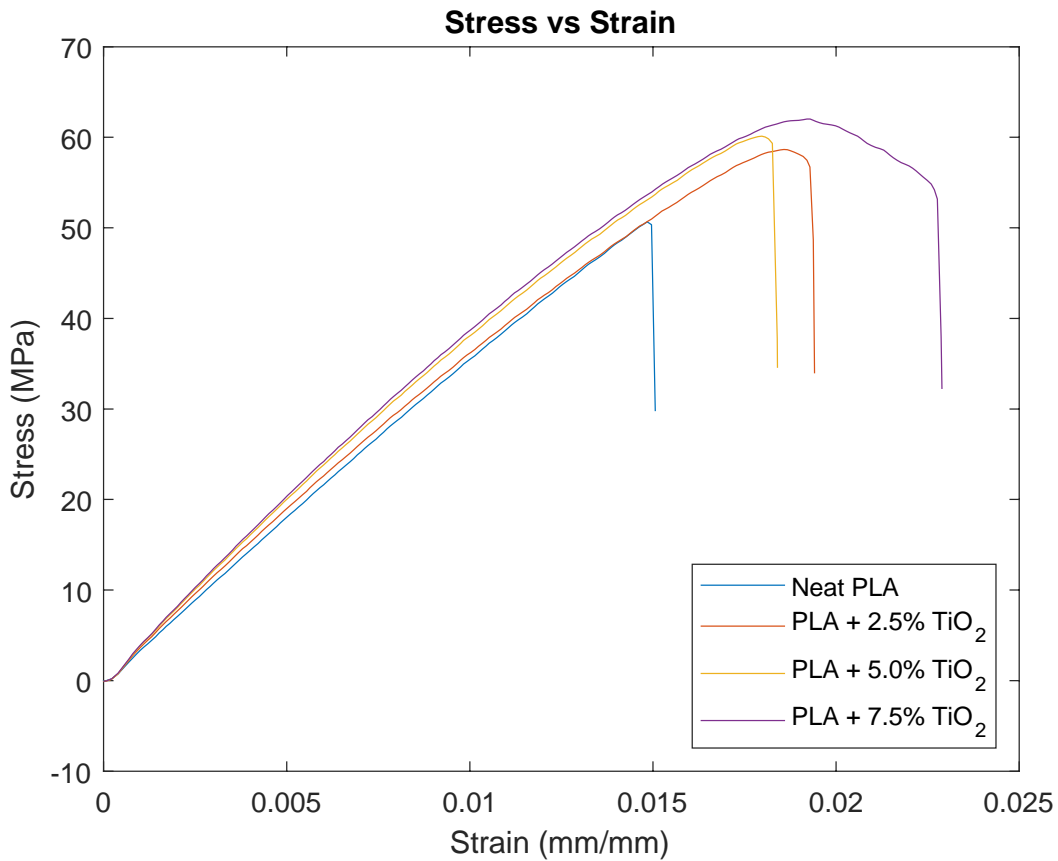


Figure 38. Tensile testing.

In addition, a statistical analysis was performed to observe the influence of the energy applied by the process and see the impact it has on the mechanical properties. As observed in Table 17, the relationship of the energy applied by ultrasound and Young's modulus is significant. According to the analysis of the energy applied to the pieces subjected to this test, on average 368.7 J is required for the neat PLA, and as nanoparticles are added, the energy decreases, reaching 276.7 J with the concentration of 7.5 wt.%. This means that as nanoparticles are added, less energy is required, and Young's modulus increases, as does, in general, for tensile strength and elongation at break. The applied energy affects the mechanical properties and significantly, the Young's modulus (Figure 39).

Table 17. Significant Parameters in Tensile Testing.

	p-value	Significant?
US Energy [J]	0.007	✓
E [MPa]	0.005	✓
σ_u[MPa]	0.639	X
ϵ_t [%]	0.663	X

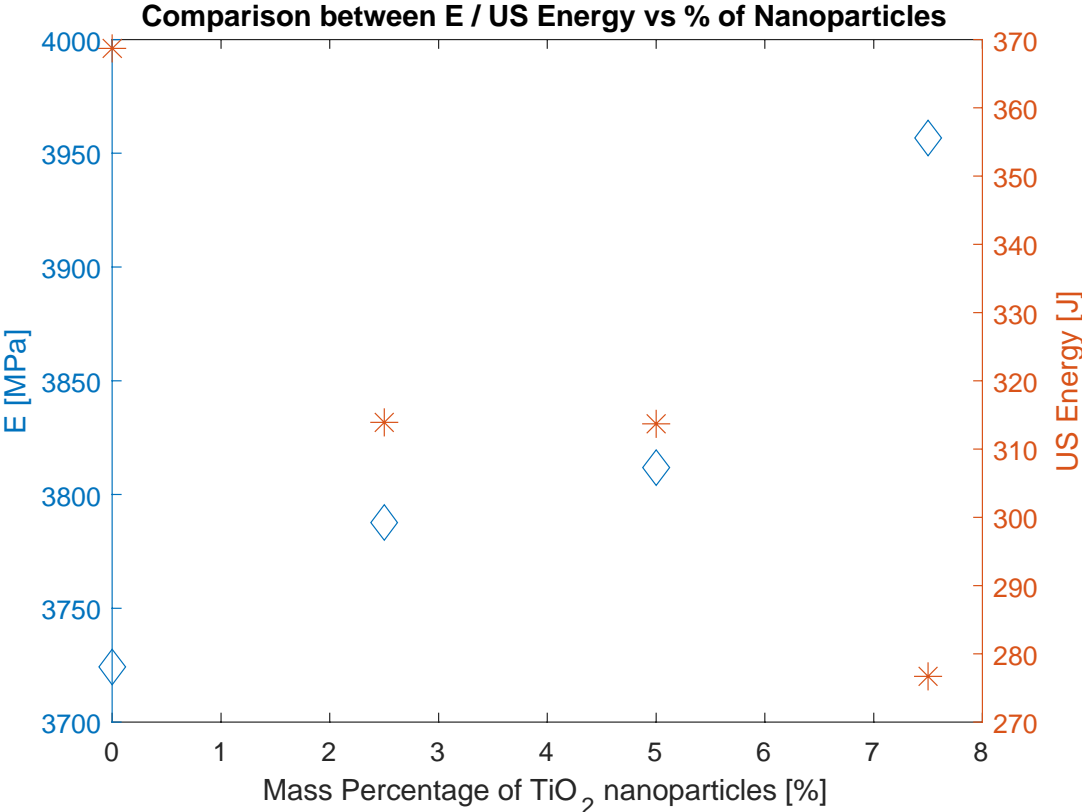


Figure 39. Young's Modulus and US Energy vs % of nanoparticles.

9. Conclusions

Ultrasonic molding is a promising technology that offers many advantages, including low costs in the use of equipment and tools, flexibility for the production of different parts, due to the ease of manufacturing molds, reduced material waste and low times of residence. Thanks to the new update offered by the Sonorus 1G machine, it was possible to establish a methodology that was validated, through two materials, which is why it represents a good strategy for obtaining a window of process parameters quickly and effectively, for any material. In addition, ultrasonic molding was found to have the ability to manufacture nanoparticle reinforced parts, PLA with TiO₂ nanoparticles, because 90% process repeatability was obtained.

As main contributions of the work, regarding the established methodology, the significant parameters obtained in the compaction, preheating and melting phases have a greater impact than in the filling phase. Furthermore, due to the variability of the process, these significant parameters may be different for each material, depending on the nature of the material. However, the expected outputs in each phase should always be the same. On the other hand, the analysis of the applied energy, allows to observe the energy range that the material requires to be a process and allows to have a greater reproducibility of the process. Finally, the percentage of parts successfully manufactured with the final process parameter windows is 90%.

The contributions by the feasibility of processing PLA / TiO₂, with the USM the TiO₂ nanoparticles are dispersed uniformly as the concentration increases. Because it is not usual behavior, more studies should be done to determine the certainty of this behavior. Likewise, the TiO₂ nanoparticles do not affect the process parameters in relation to the neat material and are not affected by their concentration variation either.

Finally, the contributions regarding the characterization of the material, with the SEM, reflects a better dispersion of nanoparticles at a higher concentration and appearance of texture that indicates rigidity. This was confirmed by increasing Young's Modulus in the Tensile Testing. With MFI, the fluidity of the material increases at a higher concentration of nanoparticles due to a possible interaction of PLA chains with TiO₂ and the decrease in agglomerates, observed in the SEM, with the increase in nanoparticles. With XRD, the TiO₂

nanoparticles in this process are in the rutile / anatase phase. With the FTIR, by increasing the concentration of nanoparticles, it affects the opacity of the polymer, therefore, it should be considered for possible application. In addition, the materials are mixed only physically, because no new bands are observed and there is no degradation of the material. With the stress test, at a higher concentration of nanoparticles, the material is stiffer due to the crystallinity provided by TiO₂.

The next steps are to complete the characterization of the pieces to obtain more concrete conclusions. These techniques include thermal property (DSC), technique for antibacterial activity, SEM to confirm nanoparticle distribution and Gel Permeation Chromatography (GPC) to confirm decrease in molecular weight. In addition, another important step is the characterization of the material without being processed to observe the influence of the ultrasound molding process. In addition, for future work, the confirmation of nanoparticle dispersion at higher concentrations due to the influence of the process must be carried out. On the other hand, carry out experimentation with a new methodology for nanoparticle dispersion (Ultrasonic dispersion or use of solvent). And once these steps are completed, search for an application for the reinforced material studied.

Appendix A

Table A.1. Abbreviations.

Abbreviations	Description
USM	Ultrasonic Molding
PA12	Polyamide 12
PLA	Poly(lactic Acid)
TiO₂	Titanium Dioxide
PP	Polypropylene
PS	Polystyrene
PMMA	Poly(Methyl Methacrylate)
UHMWPE	Ultra High Molecular Weight Polyethylene
PPSU	Polyphenylsulfone
PEEK	Polyether ether ketone
POM	Polyoxymethylene
SEM	Scanning Electron Microscopy
MFI	Melt Flow Index
XRD	X-Ray Diffraction
FTIR	Fourier Transform Infrared
GPC	Gel Permeation Chromatography
DSC	Differential Scanning Calorimetry

Appendix B

Table B.1. Variables and Symbols.

Symbol	Units	Description
AV	%	Amplitude
F	N	Force
V	mm/s	Velocity
PP	mm	Plunger Position
T	s	Time
Tr	mm	Travel
St	-	Strokes
2θ	°	Angle of reflection
US Energy	J	Ultrasonic Energy
E	MPa	Young's Modulus
σ_u	MPa	Ultimate Strength
ε_t	%	Elongation at break

Bibliography

- [1] M. Hecke and W. K. Schomburg, "Review on micro molding of thermoplastic polymers," *J. Micromechanics Microengineering*, vol. 14, no. 3, 2004, doi: 10.1088/0960-1317/14/3/R01.
- [2] W. Michaeli, A. Spennemann, and R. Gärtner, "New plastification concepts for micro injection moulding," *Microsyst. Technol.*, vol. 8, no. 1, pp. 55–57, 2002, doi: 10.1007/s00542-001-0143-9.
- [3] M. Sacristán, X. Plantá, M. Morell, and J. Puiggali, "Effects of ultrasonic vibration on the micro-molding processing of polylactide," *Ultrason. Sonochem.*, vol. 21, no. 1, pp. 376–386, 2014, doi: 10.1016/j.ultsonch.2013.07.007.
- [4] M. . Martyn, B. Whiteside, P. . Coates, P. . Allan, G. Greenway, and P. Hornsby, "Micromoulding: consideration of processing effects on medical materials," in *SPE ANTEC*, 2003.
- [5] J. . Lerma Valero, *Manual avanzado de transformación de termoplásticos por inyección: científica injection molding: recomendaciones y buenas prácticas para un proceso de inyección avanzado.*, 9th ed. Disseny, 2014.
- [6] G. Lucchetta, M. Sorgato, S. Carmignato, and E. Savio, "Investigating the technological limits of micro-injection molding in replicating high aspect ratio micro-structured surfaces," *CIRP Ann. - Manuf. Technol.*, vol. 63, no. 1, pp. 521–524, 2014, doi: 10.1016/j.cirp.2014.03.049.
- [7] M. Janer, X. Plantà, and D. Riera, "Ultrasonic moulding: Current state of the technology," *Ultrasonics*, vol. 102, no. October 2019, 2020, doi: 10.1016/j.ultras.2019.106038.
- [8] J. Chen, Y. Chen, H. Li, S. Y. Lai, and J. Jow, "Physical and chemical effects of ultrasound vibration on polymer melt in extrusion," *Ultrason. Sonochem.*, vol. 17, no. 1, pp. 66–71, 2010, doi: 10.1016/j.ultsonch.2009.05.005.
- [9] G. Chen, S. Guo, and H. Li, "Ultrasonic improvement of rheological behavior of polystyrene," *J. Appl. Polym. Sci.*, vol. 84, no. 13, pp. 2451–2460, 2002, doi: 10.1002/app.10535.
- [10] U. Heredia, E. Vázquez, I. Ferrer, C. A. Rodríguez, and J. Ciurana, "Feasibility of manufacturing low aspect ratio parts of PLA by ultrasonic moulding technology," *Procedia Manuf.*, vol. 13, pp. 251–258, 2017, doi: 10.1016/j.promfg.2017.09.065.
- [11] I. Ferrer, M. Vives-Mestres, A. Manresa, and M. L. Garcia-Romeu, "Replicability of ultrasonic molding for processing thin-wall polystyrene plates with a microchannel," *Materials (Basel)*, vol. 11, no. 8, pp. 1–18, 2018, doi: 10.3390/ma11081320.
- [12] W. Michaeli, T. Kamps, and C. Hopmann, "Manufacturing of polymer micro parts by ultrasonic plasticization and direct injection," *Microsyst. Technol.*, vol. 17, no. 2, pp. 243–249, 2011, doi: 10.1007/s00542-011-1236-8.
- [13] M. Planellas *et al.*, "Micro-molding with ultrasonic vibration energy: New method to disperse nanoclays in polymer matrices," *Ultrason. Sonochem.*, vol. 21, no. 4, pp. 1557–1569, 2014, doi: 10.1016/j.ultsonch.2013.12.027.
- [14] D. Masato, M. Babenko, B. Shriky, T. Gough, G. Lucchetta, and B. Whiteside, "Comparison of crystallization characteristics and mechanical properties of polypropylene processed by ultrasound and conventional micro-injection molding," *Int. J. Adv. Manuf. Technol.*, vol. 99, no. 1–4, pp. 113–125, 2018, doi: 10.1007/s00170-018-2493-9.
- [15] W. Michaeli and D. Opfermann, *Ultrasonic plasticising for micro injection moulding*. Woodhead Publishing Limited, 2006.
- [16] J. . Bas *et al.*, "Dispositivo ultrasónico para moldeo de micropiezas de plástico.," ES2323624A1, 2009.

- [17] F. Puliga, M. Sacristán, F. J. Plantà, and A. Navarro, "Apparatus for moulding plastics micro-pieces by ultrasounds.," US20130171287A1, 2014.
- [18] P. Negre, J. Grabalosa, I. Ferrer, J. Ciurana, A. Elías-Zúñiga, and F. Rivillas, "Study of the Ultrasonic Molding Process Parameters for Manufacturing Polypropylene Parts," *Procedia Eng.*, vol. 132, pp. 7–14, 2015, doi: 10.1016/j.proeng.2015.12.460.
- [19] C. Olmo, "Micromoldeo por ultrasónidos de ácido poliláctico: Preparación de nanocompuestos y carga con fármacos.," Universitat Politècnica de Catalunya, 2015.
- [20] A. Díaz *et al.*, "Preparation of micro-molded exfoliated clay nanocomposites by means of ultrasonic technology," *J. Polym. Res.*, vol. 21, no. 11, 2014, doi: 10.1007/s10965-014-0584-3.
- [21] C. Olmo *et al.*, "Preparation of nanocomposites of poly(ϵ -caprolactone) and multi-walled carbon nanotubes by ultrasound micro-molding. influence of nanotubes on melting and crystallization," *Polymers (Basel)*., vol. 9, no. 8, pp. 1–18, 2017, doi: 10.3390/polym9080322.
- [22] A. Díaz, M. T. Casas, and J. Puiggali, "Dispersion of functionalized silica micro- and nanoparticles into poly(nonamethylene azelate) by ultrasonic micro-molding," *Appl. Sci.*, vol. 5, no. 4, pp. 1252–1271, 2015, doi: 10.3390/app5041252.
- [23] X. Sánchez-Sánchez, A. Elías-Zuñiga, and M. Hernández-Avila, "Processing of ultra-high molecular weight polyethylene/graphite composites by ultrasonic injection moulding: Taguchi optimization," *Ultrason. Sonochem.*, vol. 44, pp. 350–358, 2018, doi: 10.1016/j.ultsonch.2018.02.042.
- [24] U. Heredia-Rivera, I. Ferrer, and E. Vázquez, "Ultrasonic molding technology: Recent advances and potential applications in the medical industry," *Polymers (Basel)*., vol. 11, no. 4, 2019, doi: 10.3390/polym11040667.
- [25] T. Dorf, I. Ferrer, and J. Ciurana, "Characterizing ultrasonic micro-molding process of polyetheretherketone (PEEK)," *Int. Polym. Process.*, vol. 33, no. 4, pp. 442–452, 2018, doi: 10.3139/217.3428.
- [26] X. Sánchez Sánchez and I. Date, "Application of ultrasonic micro injection molding for manufacturing of UHMWPE microparts.," Tecnológico de Monterrey, 2017.
- [27] T. Dorf, K. Perkowska, M. Janiszewska, I. Ferrer, and J. Ciurana, "Effect of the main process parameters on the mechanical strength of polyphenylsulfone (PPSU) in ultrasonic micro-moulding process," *Ultrason. Sonochem.*, vol. 46, no. November 2017, pp. 46–58, 2018, doi: 10.1016/j.ultsonch.2018.03.024.
- [28] X. Sánchez-Sánchez, M. Hernández-Avila, L. E. Elizalde, O. Martínez, I. Ferrer, and A. Elías-Zuñiga, "Micro injection molding processing of UHMWPE using ultrasonic vibration energy," *Mater. Des.*, vol. 132, pp. 1–12, 2017, doi: 10.1016/j.matdes.2017.06.055.
- [29] L. Rodríguez Bravo, "Microprocesado de matrices termoplásticas mediante ultrasónidos: evaluación de las propiedades químicas y físicas de los materiales procesados.," Universitat Politècnica Catalunya, 2012.
- [30] J. Grabalosa, I. Ferrer, A. Elías-Zúñiga, and J. Ciurana, "Influence of processing conditions on manufacturing polyamide parts by ultrasonic molding," *Mater. Des.*, vol. 98, pp. 20–30, 2016, doi: 10.1016/j.matdes.2016.02.122.
- [31] N. Zobeiry, "Viscoelastic constitutive models for evaluation of residual stresses in thermoset composites during cure.," The University of British Columbia, 2006.
- [32] D. Montes, "Estudi dels paràmetres del procés de micromoldeig per ultrasòns mitjançant disseny experimental.," Universitat Politècnica de Catalunya, 2016.
- [33] M. Janer, D. Montes, C. M. Rubio, X. Plantà, and M. D. Riera, "Applying ultrasonic moulding to process polyoxymethylene," *Ultrason. 2018 Proc. B.*, no. July, pp. 173–174, 2018.
- [34] A. I. Isayev, R. Kumar, and T. M. Lewis, "Ultrasound assisted twin screw extrusion of

- polymer-nanocomposites containing carbon nanotubes," *Polymer (Guildf)*., vol. 50, no. 1, pp. 250–260, 2009, doi: 10.1016/j.polymer.2008.10.052.
- [35] N. Salahuddin, M. Abdelwahab, M. Gaber, and S. Elneanaey, "Synthesis and Design of Norfloxacin drug delivery system based on PLA/TiO₂ nanocomposites: Antibacterial and antitumor activities," *Mater. Sci. Eng. C*, vol. 108, no. November 2019, 2020, doi: 10.1016/j.msec.2019.110337.
- [36] C. Man *et al.*, "Poly (lactic acid)/titanium dioxide composites: Preparation and performance under ultraviolet irradiation," *Polym. Degrad. Stab.*, vol. 97, no. 6, pp. 856–862, 2012, doi: 10.1016/j.polymdegradstab.2012.03.039.
- [37] A. Pascual, *Ultrasonic Molding Handbook*. S.L. Ultrason, 2018.
- [38] S. L. Ultrason, "No Title." .
- [39] A. Manresa, "Processat de poli(àcid làctic) (PLA) i poli(ε-caprolactona) (PCL) amb la tecnologia d'emmotllament per ultrasons (USM).," Universitat de Girona, 2018.
- [40] S. Feng, F. Zhang, S. Ahmed, and Y. Liu, "Physico-mechanical and antibacterial properties of PLA/TiO₂ composite materials synthesized via electrospinning and solution casting processes," *Coatings*, vol. 9, no. 8, 2019, doi: 10.3390/coatings9080525.
- [41] S. Mallick, Z. Ahmad, F. Touati, J. Bhadra, R. A. Shakoore, and N. J. Al-Thani, "PLA-TiO₂ nanocomposites: Thermal, morphological, structural, and humidity sensing properties," *Ceram. Int.*, vol. 44, no. 14, pp. 16507–16513, 2018, doi: 10.1016/j.ceramint.2018.06.068.
- [42] E. A. S. González, D. Olmos, M. ángel Lorente, I. Vélaz, and J. González-Benito, "Preparation and characterization of polymer composite materials based on PLA/TiO₂ for antibacterial packaging," *Polymers (Basel)*., vol. 10, no. 12, pp. 1–15, 2018, doi: 10.3390/polym10121365.
- [43] K. Thamaphat, P. Limsuwan, and B. Ngotawornchai, "Phase Characterization of TiO₂ Powder by XRD and TEM," *Kasetsart J. (Nat. Sci.)*, vol. 42, pp. 357–361, 2008.
- [44] J. Y. Zhang, I. W. Boyd, B. J. O'Sullivan, P. K. Hurley, P. V. Kelly, and J. P. Sénateur, "Nanocrystalline TiO₂ films studied by optical, XRD and FTIR spectroscopy," *J. Non. Cryst. Solids*, vol. 303, no. 1, pp. 134–138, 2002, doi: 10.1016/S0022-3093(02)00973-0.
- [45] D. Mendoza-Anaya, P. Salas, C. Angeles-Chávez, R. Pérez-Hernández, and V. M. Castaño, "Caracterización microestructural y morfología de TiO₂ para aplicaciones termoluminiscentes," *Rev. Mex. Fis.*, vol. 50, no. SUPPL., pp. 12–16, 2004.
- [46] T. Paragkumar N, D. Edith, and J. L. Six, "Surface characteristics of PLA and PLGA films," *Appl. Surf. Sci.*, vol. 253, no. 5, pp. 2758–2764, 2006, doi: 10.1016/j.apsusc.2006.05.047.
- [47] J. Sun *et al.*, "Improving performance of dental resins by adding titanium dioxide nanoparticles," *Dent. Mater.*, vol. 27, no. 10, pp. 972–982, 2011, doi: 10.1016/j.dental.2011.06.003.
- [48] S. K. Esthappan, S. K. Kuttappan, and R. Joseph, "Effect of titanium dioxide on the thermal ageing of polypropylene," *Polym. Degrad. Stab.*, vol. 97, no. 4, pp. 615–620, 2012, doi: 10.1016/j.polymdegradstab.2012.01.006.
- [49] Y. Li, C. Chen, J. Li, and X. Susan, "Synthesis and characterization of bionanocomposites of poly (lactic acid) and TiO₂ nanowires by in situ polymerization," *Polymer (Guildf)*., vol. 52, no. 11, pp. 2367–2375, 2011, doi: 10.1016/j.polymer.2011.03.050.
- [50] L. Qu *et al.*, "Industrial Crops & Products Improved mechanical and antimicrobial properties of zein / chitosan films by adding highly dispersed nano-TiO₂," *Ind. Crop. Prod.*, vol. 130, no. November 2018, pp. 450–458, 2019, doi: 10.1016/j.indcrop.2018.12.093.

Curriculum Vitae

Mariana Macías Naranjo was born in Monterrey, Nuevo León, Mexico, on November 18, 1994. She earned the Chemical Engineering degree with minor in Administration, from Instituto Tecnológico y de Estudios Superiores de Monterrey, Monterrey Campus in May 2018. In summer 2017, she studied at the University of Ljubljana, Faculty of Economics, taking two subjects.

Upon graduation, she was accepted in the program of Master in Science in Manufacturing Systems in July 2018. She earned the master degree from Instituto Tecnológico y de Estudios Superiores de Monterrey, Monterrey Campus in June 2020. Thanks to Instituto Tecnológico y de Estudios Superiores de Monterrey, she was awarded a 100% scholarship by being in a high-performance program and CONACyT provided support for living. The experimentation of the present work was carried out in Girona, Catalonia, Spain. CONACyT gave her an additional scholarship for study abroad and the University of Girona, as well as the grEp (Grup de Recerca en Enginyeria de Producte, Procés i Producció) and LEPAMAP (Laboratori d'Enginyeria Paperera i Materials Polímers) groups, were in charge of receiving the student. The student received the invitation to the doctorate from Dr. Elisa Vázquez at Instituto Tecnológico y de Estudios Superiores de Monterrey, Monterrey Campus and from Dr. Inés Ferrer at University of Girona.